isvr Institute of Sound and Vibration Research

A Fourier Technique for the Analysis of Beam-Plate Coupled Structures

J.W. Yoo, D.J. Thompson and N.S. Ferguson

ISVR Technical Memorandum No 927

January 2004

University of Southampton

SCIENTIFIC PUBLICATIONS BY THE ISVR

Technical Reports are published to promote timely dissemination of research results by ISVR personnel. This medium permits more detailed presentation than is usually acceptable for scientific journals. Responsibility for both the content and any opinions expressed rests entirely with the author(s).

Technical Memoranda are produced to enable the early or preliminary release of information by ISVR personnel where such release is deemed to the appropriate. Information contained in these memoranda may be incomplete, or form part of a continuing programme; this should be borne in mind when using or quoting from these documents.

Contract Reports are produced to record the results of scientific work carried out for sponsors, under contract. The ISVR treats these reports as confidential to sponsors and does not make them available for general circulation. Individual sponsors may, however, authorize subsequent release of the material.

UNIVERSITY OF SOUTHAMPTON

INSTITUTE OF SOUND AND VIBRATION RESEARCH

DYNAMICS GROUP

A Fourier Technique for the Analysis of Beam-Plate Coupled Structures

by

J.W. Yoo, D.J. Thompson and N.S. Ferguson

ISVR Technical Memorandum No: 927

January 2004

CONTENTS

1. INTRODUCTION

The dynamical behaviour of a coupled structure consisting of a single beam and a plate was analysed previously [1], by using a wave approach. Subsequently the approach was developed to obtain the response of a beam - plate - beam structure.

In the wave method, the structural behaviour was calculated based on the free wavenumber of a substructure. It was assumed that the beam was much stiffer than the plate, that is, the free wavenumber of the plate was assumed to be sufficiently larger than that of the uncoupled beam. From this assumption, using an approximate plate impedance, the coupled beam wavenumber could be obtained iteratively.

The wave method generally showed reasonable results. Nevertheless, there were some difficulties. For example, if the coupled beam wavenumber becomes close to the plate wavenumber, then the iterative method used is no longer applicable. Furthermore, when the coupled beam wavenumber becomes larger than that of the plate, then it is difficult to consider the corresponding plate wavenumber, which will be changed from a travelling wavenumber to a nearfield wavenumber. Also, the travelling wave and the nearfield wave of the coupled beam were considered separately and this separation technique results in a violation of energy conservation for the plate, which still remains a problem to be overcome.

Although the behaviour of the two-beam structure in a symmetric configuration was analysed using the wave method, it would be difficult to extend this to obtain the response when it is not in an exact symmetric configuration, for example when the thicknesses of the two beams are different. This is because its behaviour is calculated based on anti-symmetric and symmetric responses of the single beam-plate structure which cannot represent the more general case.

Considering these difficulties, it is necessary to consider a more general and less restrictive method to replace the wave method. Ji et al. [2] described the Fourier transform method for the analysis of the coupled structure consisting of a beam and plate. As this method considers all possible values for the wavenumber k_x, it is expected that the difficulties of the wave method, such as the assumption about the wavenumber and the related approximate impedance, can be avoided. In addition, the travelling wave and the nearfield wave of the coupled beam need not be considered separately, and the relationship between the beams and the plate of a two-beam structure can be directly determined for the case when the thicknesses of the beams are different.

As in the previous report [1], it is assumed that the beam attached to the plate has infinite torsional stiffness. A sliding condition is considered at the ends of the beam for compatibility with proposed future study of a four-beam structure. It had been assumed previously [1, 3] that the neutral axis of the beam lies at the bottom of the beam. Because of this, a small difference in the mobility between analytical and Finite Element results was observed, especially at high frequencies. Although more study is necessary to correct this difference, here it is assumed that the beam neutral axis lies in the centre of the beam. This is more convenient for comparing the accuracy of the present analysis with FE analysis, without any additional complexity in the research.

The report can be divided into three parts based on the configuration of the structure and the location of an external force. In sections 2, 3, and 4, the coupled structure consisting of a beam and a plate is examined for excitation on the beam. Section 5 describes the coupled structure consisting of a beam and a plate, where the plate is excited. Then, a beam-plate-beam coupled structure is presented and analysed in section 6.

In detail, for the case where the beam is excited, the structural behaviour is presented for the coupled structure consisting of an infinite single beam and a semi-infinite plate using the Fourier transform method. The dynamic characteristics of the structure are examined in terms of the spatial Fourier transformed response and some physical meanings are given. Both numerical quadrature and FFT implementations of the Fourier transform are considered.

Following this, a Fourier series is applied to obtain the response of a finite beam coupled to a finite plate. Subsequently the Fourier series method is applied to the case where the plate is excited in the beam-plate coupled structure and finally to the case where two beams are attached to a finite plate.

The results of the analysis are compared and validated against those obtained using the FEM. Furthermore, power relationships based on the Fourier transform method are presented and some comments are given on comparisons with results based on the previous wave method.

2. INFINITE BEAM COUPLED TO SEMI-INFINITE PLATE: BEAM-EXCITED

2.1 Structural coupling

2.1.1 Wavenumber relationship

Consider a built-up structure consisting of an infinite beam and a plate of semi-infinite width and infinite length shown in Figure 1. Harmonic motion at frequency ω is assumed throughout with a time dependence of $e^{i\omega t}$. It is assumed that the beam is infinitely stiff to torsion along $y = 0$.

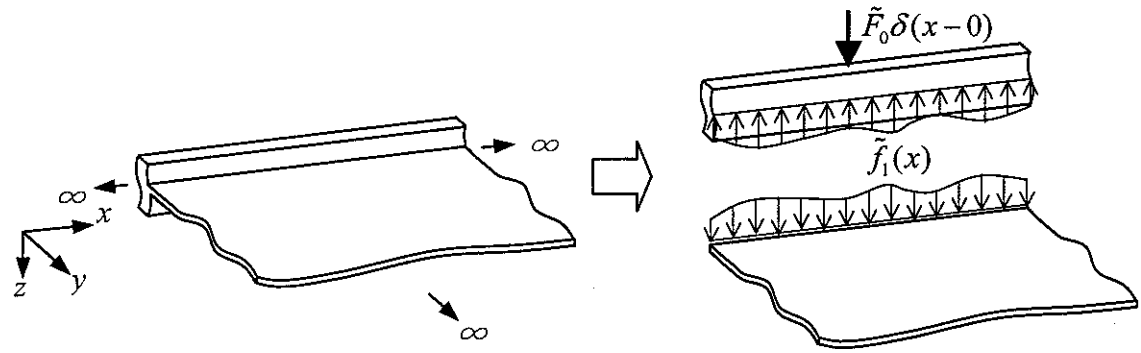

Figure 1. A built-up structure consisting of an infinite beam attached to a semi-infinite width plate.

Firstly, considering the uncoupled free wave motion of the beam at frequency ω, the relevant equation of motion of the beam with damping is

$$\tilde{D}_b \frac{d^4 \tilde{w}_b(x)}{dx^4} - m_b' \omega^2 \tilde{w}_b(x) = 0 \qquad (2.1)$$

where $\tilde{w}_b$ is the complex displacement amplitude of the beam vibration, $\tilde{D}_b$ is the bending stiffness given by $\tilde{E}_b I$, with $\tilde{E}_b \left(= E_b\left(1 + i\eta_b\right)\right)$ Young's modulus with damping, I the second moment of area of the beam and m_b' is the mass per unit length.

When the semi-infinite plate and the infinite beam are joined along the line $y = 0$, a force per unit length $\tilde{f}_1(x)$ acts between them as shown in Figure 1. An external force acting on the beam is defined by a point force $\tilde{F}_0\delta(x-0)$ where $\delta(x-0)$ represents a delta function acting at $x = 0$. Then equation (2.1) becomes

$$\tilde{D}_b \frac{d^4 \tilde{w}_b(x)}{dx^4} - m_b' \omega^2 \tilde{w}_b(x) = \tilde{F}_0 \delta(x-0) - \tilde{f}_1(x) \tag{2.2}$$

Spatial Fourier transform pairs are defined by the relationship between the coordinate x and real wavenumber k_x in the x direction as follows.

$$\tilde{W}_b(k_x) = \int_{-\infty}^{\infty} \tilde{w}_b(x) e^{-ik_x x} dx . \tag{2.3}$$

$$\tilde{w}_b(x) = \frac{1}{2\pi} \int_{-\infty}^{\infty} \tilde{W}_b(k_x) e^{ik_x x} dk_x . \tag{2.4}$$

For spatial derivatives of the functions one has

$$\begin{aligned} ik_x \tilde{W}_b(k_x) &= \int_{-\infty}^{\infty} \frac{d\tilde{w}_b(x)}{dx} e^{-ik_x x} dx . \\ -k_x^2 \tilde{W}_b(k_x) &= \int_{-\infty}^{\infty} \frac{d^2 \tilde{w}_b(x)}{dx^2} e^{-ik_x x} dx . \end{aligned} \tag{2.5a,b}$$

Therefore, the spatial Fourier transform of equation (2.2) gives

$$\tilde{D}_b k_x^4 \tilde{W}_b(k_x) - m_b' \omega^2 \tilde{W}_b(k_x) = \tilde{F}_0 - \tilde{F}_1(k_x) . \tag{2.6}$$

where $\tilde{F}_1(k_x)$ is the Fourier transform of $\tilde{f}_1(x)$.

The equation of motion of the free plate with damping is

$$\tilde{D}_p \left(\frac{\partial^4 \tilde{w}_p(x,y)}{\partial x^4} + 2 \frac{\partial^4 \tilde{w}_p(x,y)}{\partial x^2 \partial y^2} + \frac{\partial^4 \tilde{w}_p(x,y)}{\partial y^4} \right) - m_p'' \omega^2 \tilde{w}_p(x,y) = 0 \tag{2.7}$$

where $\tilde{D}_p$ is the plate bending stiffness given by $\tilde{D}_p = \tilde{E}_p h^3 / 12(1-\nu^2)$, ν is Poisson's ratio, h is the thickness and m_p'' is the mass per unit area of the plate. This leads to free wave solutions with wavenumber $\tilde{k}_p^4 = m_p'' \omega^2 / \tilde{D}_p$.

If the motion of the plate is defined by a wavenumber k_x in the x direction, the response can be written as $\tilde{W}_p(k_x, y)$. The complete response at position y can thus be given by the Fourier transform

$$\tilde{w}_p(x,y) = \frac{1}{2\pi} \int_{-\infty}^{\infty} \tilde{W}_p(k_x, y) e^{ik_x x} dk_x , \tag{2.8}$$

which has an inverse Fourier transform

$$\tilde{W}_p(k_x, y) = \int_{-\infty}^{\infty} \tilde{w}_p(x, y) e^{-ik_x x} dx \,. \tag{2.9}$$

Now the Fourier transform of equation (2.7) is

$$\tilde{D}_p \left\{ k_x^4 \tilde{W}_p(k_x, y) - 2k_x^2 \frac{\partial^2 \tilde{W}_p(k_x, y)}{\partial y^2} + \frac{\partial^4 \tilde{W}_p(k_x, y)}{\partial y^4} \right\} - m_p'' \omega^2 \tilde{W}_p(k_x, y) = 0 \,. \tag{2.10}$$

Since $\tilde{k}_p^4 = m_p'' \omega^2 / \tilde{D}_p$, this can be written as

$$k_x^4 \tilde{W}_p(k_x, y) - 2k_x^2 \frac{\partial^2 \tilde{W}_p(k_x, y)}{\partial y^2} + \frac{\partial^4 \tilde{W}_p(k_x, y)}{\partial y^4} - \tilde{k}_p^4 \tilde{W}_p(k_x, y) = 0 \,. \tag{2.11}$$

Suppose that the solution for the harmonic wave in the plate becomes

$$\tilde{W}_p(k_x, y) = \tilde{B} e^{\tilde{k}_y y} \tag{2.12}$$

where $\tilde{k}_y$ is the trace wavenumber for the wave radiating into the plate normal to the beam. Substituting equation (2.12) into equation (2.11) gives

$$k_x^4 - 2k_x^2 \tilde{k}_y^2 + \tilde{k}_y^4 - \tilde{k}_p^4 = 0 \,.$$

$$\tilde{k}_y^2 = k_x^2 \pm \tilde{k}_p^2 \,. \tag{2.13}$$

Therefore, if the negative square root is assumed for waves propagating or decaying away from the junction, two different types of wavenumber in the plate are found to be

$$\tilde{k}_y = -\sqrt{k_x^2 - \tilde{k}_p^2} = \tilde{k}_{y1} \,, \tag{2.14a}$$

$$\tilde{k}_y = -\sqrt{k_x^2 + \tilde{k}_p^2} = \tilde{k}_{y2} \,. \tag{2.14b}$$

If $|k_x| < |\tilde{k}_p|$, then wavenumber $\tilde{k}_{y1}$ may be considered to represent a wave propagating outward into the plate (if k_p is real then k_{y1} is imaginary for $k_x < k_p$) and $\tilde{k}_{y2}$ is considered

as a nearfield wave decaying outward from the beam. Conversely, if $|k_x| > |\tilde{k}_p|$, then both may be considered as nearfield waves.

Consequently the travelling and nearfield waves for the plate can be written as

$$\tilde{W}_p(k_x, y) = \tilde{B}e^{\tilde{k}_{y1}y} + \tilde{C}e^{\tilde{k}_{y2}y}. \tag{2.15}$$

2.1.2 Response of the coupled beam

As the wavenumber relationship of the coupled structure is presented, the response of the structure can be obtained from boundary conditions. The boundary conditions when a semi-infinite plate is attached at its edge to the beam are:

(i) Continuity equation; equal displacement

$$\tilde{W}_b(k_x) = \tilde{W}_p(k_x, y)\Big|_{y=0} \tag{2.16}$$

(ii) Sliding condition for the plate; for simplicity the beam is assumed infinitely stiff to torsion along y=0

$$\left.\frac{\partial \tilde{W}_p(k_x, y)}{\partial y}\right|_{y=0} = 0 \tag{2.17}$$

(iii) Force equilibrium condition; the force on the plate is equal and opposite to the force on the beam

$$\tilde{D}_p\left[\frac{\partial^3 \tilde{W}_p(k_x, y)}{\partial y^3} - k_x^2(2-\nu)\frac{\partial \tilde{W}_p(k_x, y)}{\partial y}\right]_{y=0} = \tilde{F}_1(k_x). \tag{2.18}$$

From boundary condition (i),

$$\tilde{W}_b(k_x) = \tilde{W}_p(k_x, y)\Big|_{y=0} = \tilde{B} + \tilde{C} \tag{2.19}$$

From boundary condition (ii),

$$\left.\frac{\partial \tilde{W}_p(k_x, y)}{\partial y}\right|_{y=0} = \tilde{B}\tilde{k}_{y1} + \tilde{C}\tilde{k}_{y2} = 0, \tag{2.20}$$

and therefore,

$$\tilde{B} = -\frac{\tilde{k}_{y2}}{\tilde{k}_{y1}}\tilde{C}. \tag{2.21}$$

Equation (2.19) for the boundary condition (i) becomes

$$\tilde{W}_b(k_x) = \left(1 - \frac{\tilde{k}_{y2}}{\tilde{k}_{y1}}\right)\tilde{C}. \tag{2.22}$$

From equations (2.18) and (2.20),

$$\tilde{F}_1(k_x) = \tilde{D}_p\left[\frac{\partial^3 \tilde{W}_p(k_x, y)}{\partial y^3}\right]_{y=0} = \tilde{D}_p\left(\tilde{B}\tilde{k}_{y1}^3 + \tilde{C}\tilde{k}_{y2}^3\right). \tag{2.23}$$

Substituting equation (2.21) into equation (2.23) gives

$$\tilde{F}_1(k_x) = \tilde{D}_p\left[-\frac{\tilde{k}_{y2}}{\tilde{k}_{y1}}\tilde{C}\tilde{k}_{y1}^3 + \tilde{C}\tilde{k}_{y2}^3\right] = \tilde{D}_p\tilde{k}_{y2}\left(\tilde{k}_{y1} + \tilde{k}_{y2}\right)\left(-\tilde{k}_{y1} + \tilde{k}_{y2}\right)\tilde{C}.$$

$$\tilde{F}_1(k_x) = -\tilde{D}_p\tilde{k}_{y1}\tilde{k}_{y2}\left(\tilde{k}_{y1} + \tilde{k}_{y2}\right)\left(1 - \frac{\tilde{k}_{y2}}{\tilde{k}_{y1}}\right)\tilde{C}. \tag{2.24}$$

From equation (2.22), equation (2.24) can be expressed in terms of $\tilde{W}_b(k_x)$ as follows.

$$\tilde{F}_1(k_x) = -\tilde{D}_p\tilde{k}_{y1}\tilde{k}_{y2}\left(\tilde{k}_{y1} + \tilde{k}_{y2}\right)\tilde{W}_b(k_x). \tag{2.25}$$

Note that from equation (2.25), an impedance term can be derived as follows.

$$\tilde{Z}'_p(k_x) = \frac{\tilde{F}_1(k_x)}{i\omega\tilde{W}_b(k_x)} = -\frac{\tilde{D}_p}{i\omega}\tilde{k}_{y1}\tilde{k}_{y2}\left(\tilde{k}_{y1} + \tilde{k}_{y2}\right). \tag{2.26}$$

where $\tilde{Z}'_p(k_x)$ represents the exact line impedance of the plate acting on the beam for the wavenumber k_x. Equation (2.6), representing motion of the coupled structure, becomes, on substituting for the interaction force

$$\tilde{W}_b(k_x)\left[\tilde{D}_b k_x^4 - m'_b\omega^2 - \tilde{D}_p\tilde{k}_{y1}\tilde{k}_{y2}\left(\tilde{k}_{y1} + \tilde{k}_{y2}\right)\right] = \tilde{F}_0, \tag{2.27}$$

which can be written as

$$\tilde{W}_b(k_x) = \frac{\tilde{F}_0}{\tilde{D}_b k_x^4 - m'_b\omega^2 - \tilde{D}_p\tilde{k}_{y1}\tilde{k}_{y2}\left(\tilde{k}_{y1} + \tilde{k}_{y2}\right)}. \tag{2.28}$$

Because the uncoupled beam wavenumber is given by $\tilde{k}_b^4 = m_b'\omega^2/\tilde{D}_b$, this equation can be re-expressed as

$$\tilde{W}_b(k_x) = \frac{\tilde{F}_0/\tilde{D}_b}{k_x^4 - \tilde{k}_b^4 - \tilde{D}_p\tilde{k}_{y1}\tilde{k}_{y2}\left(\tilde{k}_{y1}+\tilde{k}_{y2}\right)/\tilde{D}_b}. \tag{2.29}$$

The displacement of the beam at position x is given by the inverse Fourier transform equation (2.4) which gives

$$\tilde{w}_b(x) = \frac{\tilde{F}_0}{2\pi\tilde{D}_b}\int_{-\infty}^{\infty}\frac{1}{k_x^4 - \tilde{k}_b^4 - \tilde{D}_p\tilde{k}_{y1}\tilde{k}_{y2}\left(\tilde{k}_{y1}+\tilde{k}_{y2}\right)/\tilde{D}_b}e^{ik_x x}dk_x. \tag{2.30}$$

Note that as equation (2.30) includes the uncoupled beam wavenumber $\tilde{k}_b$, the meaningful range of k_x for the integral depends on the uncoupled wavenumber $\tilde{k}_b$, as will be shown later. By introducing a new variable γ, defined as the ratio of the coupled wavenumber k_x to the uncoupled real wavenumber k_b ($\gamma = k_x/k_b$), consideration of both k_x and k_b can be simplified.

If the denominator of equation (2.30) is divided by k_b^4, then equation (2.30) becomes

$$\tilde{w}_b(x) = \frac{\tilde{F}_0}{2\pi\tilde{D}_b k_b^4}\int_{-\infty}^{\infty}\frac{1}{k_x^4/k_b^4 - \tilde{k}_b^4/k_b^4 - \tilde{D}_p\tilde{k}_{y1}\tilde{k}_{y2}\left(\tilde{k}_{y1}+\tilde{k}_{y2}\right)/\left(\tilde{D}_b k_b^4\right)}e^{ik_x x}dk_x. \tag{2.31}$$

Also, as the plate wavenumbers $\tilde{k}_{y1}$ and $\tilde{k}_{y2}$ include the wavenumber k_x, another variable is introduced as follows.

$$\xi = \frac{k_b}{\tilde{k}_p}. \tag{2.32}$$

Then, as $\gamma\xi = k_x/\tilde{k}_p$, the third term of the denominator of equation (2.31) is

$$\begin{aligned}
&-\tilde{D}_p\tilde{k}_{y1}\tilde{k}_{y2}\left(\tilde{k}_{y1}+\tilde{k}_{y2}\right)/\left(\tilde{D}_b k_b^4\right)\\
&= \tilde{D}_p\tilde{k}_p^3\sqrt{(\gamma\xi)^4-1}\left(\sqrt{(\gamma\xi)^2-1}+\sqrt{(\gamma\xi)^2+1}\right)/\left(\tilde{D}_b k_b^4\right)\\
&= m_p''\sqrt{(\gamma\xi)^4-1}\left(\sqrt{(\gamma\xi)^2-1}+\sqrt{(\gamma\xi)^2+1}\right)/\left[m_b'\tilde{k}_p\left(1+i\eta_b\right)\right].
\end{aligned} \tag{2.33}$$

To simplify, if new variables ϕ and ψ are given by

$$\phi = \sqrt{(\gamma\xi)^2 + 1}\,,\ \psi = \sqrt{(\gamma\xi)^2 - 1}\,,\ \mu = m_p'' \big/ \left(m_b' \tilde{k}_p\right) \tag{2.34}$$

then, equation (2.33) becomes

$$-\tilde{D}_p \tilde{k}_{y1} \tilde{k}_{y2} \left(\tilde{k}_{y1} + \tilde{k}_{y2}\right) \big/ \left(\tilde{D}_b k_b^4\right) = \mu\phi\psi(\phi + \psi) / (1 + i\eta_b)\,. \tag{2.35}$$

Thus, assuming small damping $\tilde{k}_b^4 / k_b^4 \approx 1 - i\eta_b$, equation (2.31) becomes

$$\tilde{w}_b(x) \simeq \frac{\tilde{F}_0}{2\pi \tilde{D}_b k_b^3} \int_{-\infty}^{\infty} \frac{e^{ik_b x\gamma} d\gamma}{\gamma^4 - (1 - i\eta_b) + \mu\phi\psi(\phi + \psi)(1 - i\eta_b)} \tag{2.36}$$

2.2 Discussion

If the plate is removed from the beam, then the third term of the denominator of equation (2.30) is equal to zero, and the response should be that of a forced uncoupled beam. Then, the corresponding equation becomes

$$\tilde{w}_b(x) = \frac{\tilde{F}_0}{2\pi \tilde{D}_b} \int_{-\infty}^{\infty} \frac{e^{ik_x x}}{k_x^4 - \tilde{k}_b^4} dk_x\,. \tag{2.37}$$

If the non-dimensional wavenumber $\gamma (= k_x / k_b)$ is used, then equation (2.37) becomes

$$\tilde{w}_b(x) = \frac{\tilde{F}_0}{2\pi \tilde{D}_b k_b^3} \int_{-\infty}^{\infty} \frac{e^{ik_b x\gamma} d\gamma}{\gamma^4 - (1 - i\eta_b)}\,. \tag{2.38}$$

The solution for equation (2.37) can be obtained analytically. First of all, note that the integrand has four poles at $k_x = \pm\tilde{k}_b$ and $\pm i\tilde{k}_b$ which are complex numbers. Accordingly, they can be presented in the complex plane as shown in Figure 2. For the case when $x > 0$, the function $e^{ik_x x}$ goes to zero as $\mathrm{Im}(k_x) \to +\infty$ in the figure, so the contour should be closed in the upper half plane (anticlockwise) as shown in the figure. Therefore, contour integration can be applied in this upper half plane.

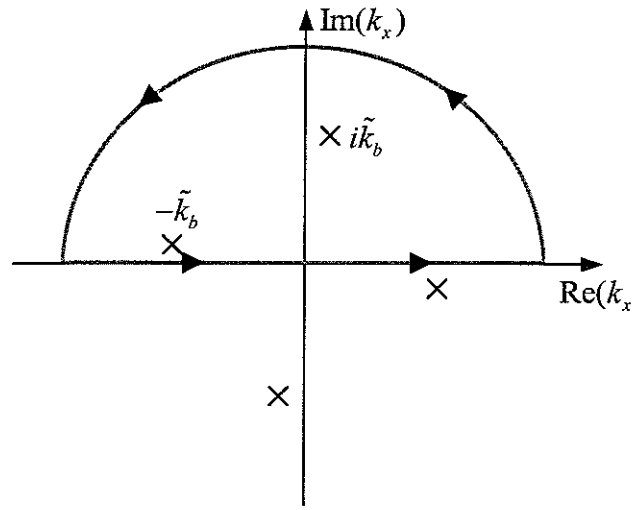

Figure 2. Poles of the uncoupled beam and the path of the corresponding contour integral.

As the poles are at complex values of k_x, it can be seen that the contour encloses only two poles, $k_x = i\tilde{k}_b$ and $-\tilde{k}_b$. Then, the integral can be evaluated using the residue theorem [4] as

$$\int_C f(z)\,dz = 2\pi i \sum_{j=1}^{m} \operatorname*{Res}_{z=a_j} f(z) \tag{2.39}$$

for poles a_1, a_2, $\cdots$, a_m inside path C. Also, any residue of the function $f(z) = p(z)/q(z)$ with simple poles can be obtained by [4]

$$\operatorname*{Res}_{z=a} f(z) = \operatorname*{Res}_{z=a} \frac{p(z)}{q(z)} = \frac{p(a)}{q'(a)}. \tag{2.40}$$

By the residue theorem,

$$\int_{-\infty}^{\infty} \frac{e^{ik_x x}}{k_x^4 - \tilde{k}_b^4}\,dk_x = 2\pi i \sum \operatorname{Res}\left(\frac{e^{ik_x x}}{k_x^4 - \tilde{k}_b^4}\right) = \frac{2\pi}{4\tilde{k}_b^3}\left(-e^{-\tilde{k}_b x} - ie^{-i\tilde{k}_b x}\right). \tag{2.41}$$

as the contribution from the semi-circular arc on the contour can be shown to be equal to zero. Finally, the analytical solution for the forced uncoupled beam is

$$\tilde{w}_b(x) = \frac{\tilde{F}_0}{\tilde{D}_b 4\tilde{k}_b^3}\left(-e^{-\tilde{k}_b x} - ie^{-i\tilde{k}_b x}\right),\ x \geq 0 \tag{2.42}$$

which is the well-known solution for the forced infinite beam [5].

The Fourier transform method, such as given by equation (2.37), can be compared with the wave approach. In the wave approach, the coupled beam wavenumber k_x is calculated based on the free (damped) beam wavenumber. Meanwhile, in the Fourier

transform method, it is necessary to consider all possible real values of the wavenumber k_x. As can be seen in equation (2.37), the denominator is minimized when $k_x = k_b$, and correspondingly the beam response will have a peak at this wavenumber. Thus, it can now be clear how the two methods differ. Whilst free wavenumbers and only their related coupled wavenumber k_x are considered in the wave method, in the Fourier transform method, the whole range of real values for the wavenumber k_x are included in the integral.

In the same manner, equation (2.30) shows how the response of the beam can be obtained from the inverse Fourier transform over wavenumber k_x for the case when the plate is attached to the beam. The Fourier transformed beam response will be maximum when $k_x \approx k_b$ although the exact value depends on the third term of the denominator.

The physical meaning of the third term can be identified in equation (2.36). Assuming the beam and the plate are undamped, and if $|k_x| \ll |k_p|$, then the third term is approximately

$$\mu\phi\psi(\phi+\psi) = \frac{m_p''(-1+i)}{m_b' k_p}. \tag{2.43}$$

Thus this complex term introduces damping to the beam as well as a mass effect. That is, the imaginary part in the displacement response has a damping-like effect. Also, the real part can be regarded as mass-like term and will shift the peak response to a wavenumber slightly above k_b. This is the same physical behaviour as explained and described previously [3]. If $m_b' \ll m_p''/k_p$ then the effect of this term will be small. In fact, m_p''/k_p is the mass, per unit length along the beam, of a plate having a width of approximately one-sixth of the plate wavelength [6]. Therefore, its effect becomes small as frequency increases due to the factor $1/k_p$. This influence will be mentioned again in the section containing numerical results and discussion.

2.3 Numerical analysis

2.3.1 Uncoupled beam in wavenumber domain

Before numerical analysis is carried out for the coupled structure shown in Figure 1, it is worthwhile to consider an uncoupled infinite beam. The response of the uncoupled beam can be simply obtained from equation (2.37). The dimensions of the uncoupled beam chosen are those presented in Table 1.

Table 1. Dimensions of the uncoupled beam.

Material	Perspex
Young's modulus, E (GNm^{-2})	4.4
Poisson's ratio, ν	0.38
Density, ρ (kgm^{-3})	1152.0
Thickness, t (mm)	5.9
Height of the beam, h (mm)	68.0
Loss factor of the beam, η_b	0.05

The external point force $\tilde{F}_0 = 1$ is applied at $x = 0$ on the infinite beam. Although, to obtain the exact response, it is necessary to consider the whole range of the wavenumber, from $-\infty$ to ∞ as presented in equation (2.37), this is not possible in a numerical integral. Therefore, initially the range of the wavenumber k_x is chosen to lie between -100 and $+100$ rad/m. Then $\tilde{W}_b(k_x)$ can be evaluated for different values of k_x and k_b when the third term of the denominator of equation (2.28) equals zero. The modulus of the transformed displacement of the uncoupled beam based on equation (2.28) is shown in Figure 3 for a frequency of 10 Hz.

Figure 3 shows that the response of the uncoupled beam as a function of the wavenumber k_x is symmetric in shape. The pole of equation (2.28) at 10 Hz is identified at $k_x = \pm 1.3$ rad/m because the uncoupled wavenumber k_b is 1.3 rad/m at this frequency, minimising the denominator. Note, in fact, that the pole lies in the complex plane near this value of k_x. This leads to a peak in $\left|\tilde{W}_b(k_x)\right|$ at this value of k_x.

The correct response of the beam displacement $\tilde{w}_b(x)$ is obtained when all possible responses shown in Figure 3 are considered in equation (2.30). Note that there is also some response not shown at $|k_x| > 100$, although it is small. However, truncating the integral at $k_x = \pm 100$ rad/m appears to be justified from the low response levels and contribution at these values of k_x.

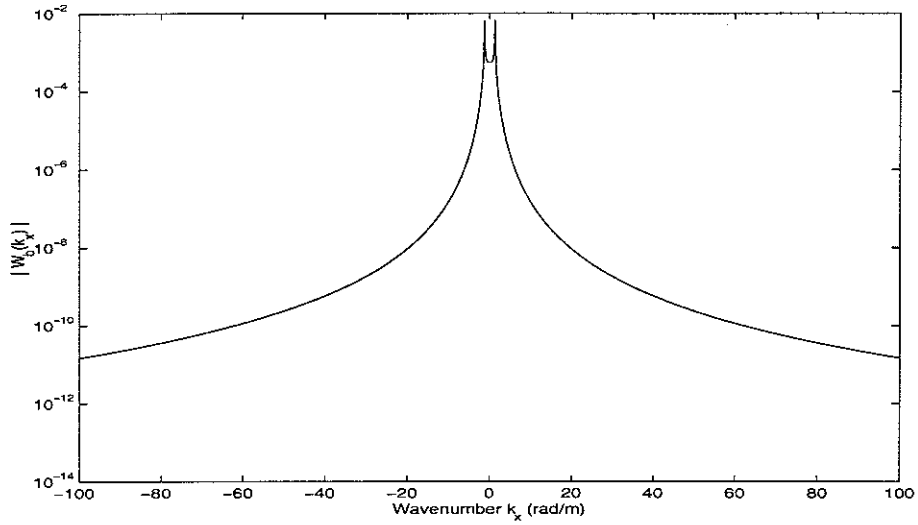

Figure 3. Fourier transformed displacement of the uncoupled beam at 10 Hz. $k_b = 1.3$ rad/m.

Figure 4 shows the Fourier transformed displacement of the uncoupled beam at 1 kHz. The corresponding pole occurs at $k_x = \pm 12.8$ rad/m. It should be noted that the peaks at the pole do not tend to infinity due to the damping of the beam itself. Also, note that the uncoupled beam wavenumber k_b depends on frequency.

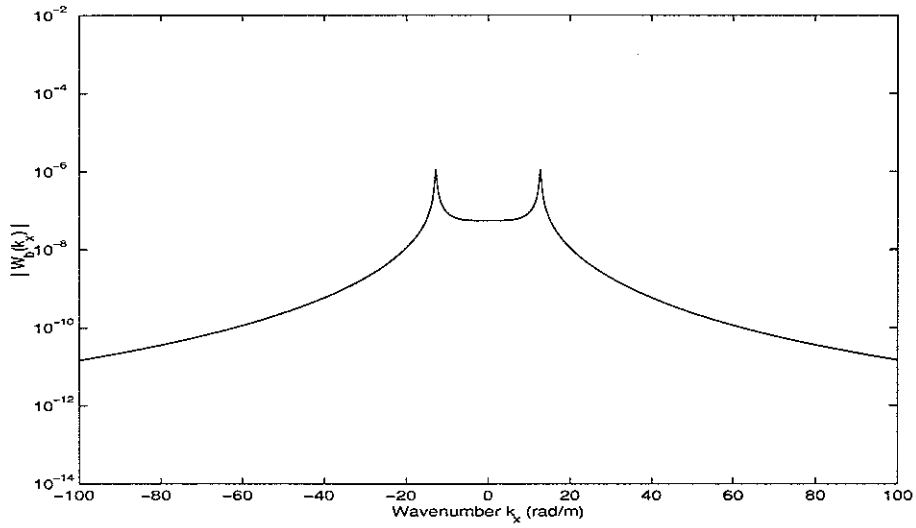

Figure 4. Fourier transformed displacement of the uncoupled beam at 1 kHz. $k_b = 12.8$ rad/m.

2.3.2 Uncoupled beam: Fourier transform

As the Fourier transformed response is presented, the forced frequency response function can be obtained based on equation (2.37). Also, as the wave solution for the forced uncoupled beam is analytically presented in equation (2.42), it will be helpful to compare results from these two equations. In order to evaluate the integral, the function QUADL [7] of MATLAB was used, which is programmed by using an adaptive Lobatto quadrature.

As explained before, it is not possible to include the whole range of the wavenumber from $-\infty$ to ∞ in equation (2.37). Therefore, it seems necessary to infer an appropriate wavenumber range to be considered. Because the uncoupled beam wavenumber k_b depends on frequency, it seems more reasonable to use equation (2.38) including the non-dimensional wavenumber $\gamma(=k_x/k_b)$ to find the wavenumber range. In Figure 5, the inverse Fourier transformed results depending on the different ranges of the non-dimensional wavenumber are compared with the analytical result based on equation (2.42). These show the response at the point of excitation.

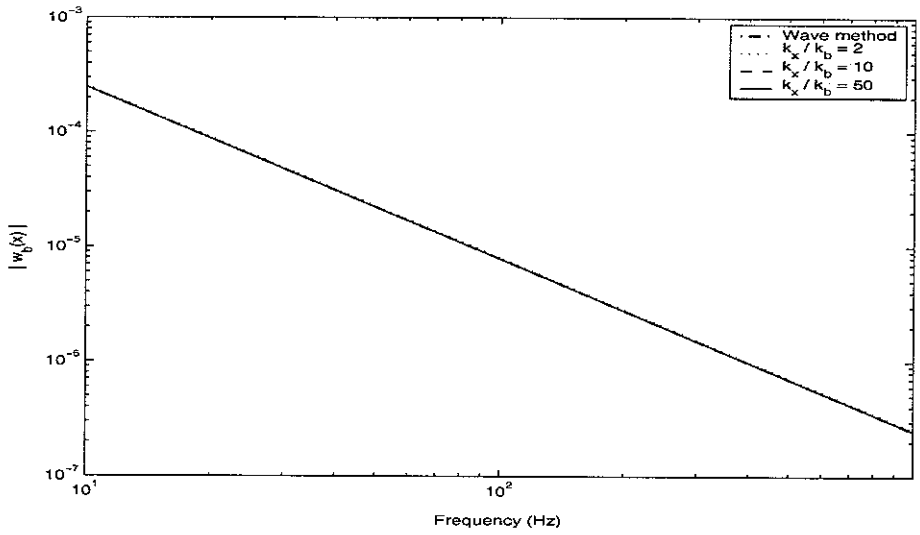

Figure 5. Displacement of the uncoupled infinite beam at the excitation point when different ranges of non-dimensional wavenumber γ are considered.

As can be seen, the inverse Fourier transformed response for the case $-2 \le \gamma \le 2$ is already close to the analytical result, with an error of 2.7%. When γ is considered from -50 to $+50$, the error is approximately 0.0001 %. Therefore, it can be said that $-50 \le \gamma \le 50$ is an

acceptable range for evaluating the forced response of the uncoupled beam, which shows consistency with the following case when a coupled beam is investigated.

2.3.3 Coupled beam in wavenumber domain

Now, attaching the semi-infinite plate to the beam, one can compare how the response is changed. The material and all dimensions are the same as presented in Table 1. The thickness of the plate is 5.9 mm and the loss factor η_p is 0.05. The second moment of area of the beam cross section is calculated by assuming that the beam is located symmetrically with respect to the plate, i.e. that its neutral axis lies in the centre of the beam, $I = th^3/12$.

In order to examine the relationship between the response of the coupled beam and the wavenumber k_x, the response $\tilde{W}_b(k_x)$ corresponding to k_x is first presented using equation (2.28). Figure 6 shows the modulus of the transformed displacement of the coupled beam for a frequency of 10 Hz.

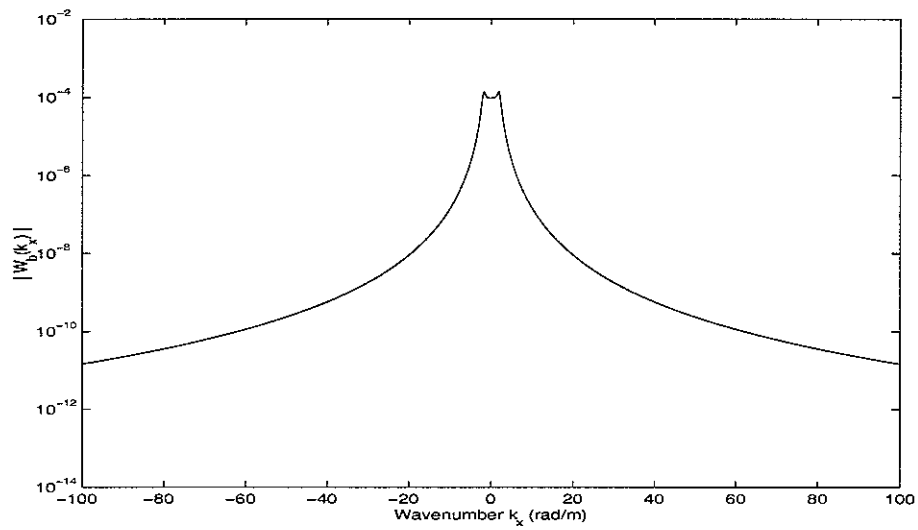

Figure 6. Fourier transformed displacement of the coupled beam as in Figure 1 at 10 Hz. $k_b = 1.3$ rad/m. $m_p''/\left(m_b' k_p\right) = 3.5$.

Comparing Figures 3 and 6, it is clear that the coupled beam is influenced by the damping effect of the plate near the peaks. While the uncoupled wavenumber $k_b = 1.3$ rad/m, the pole of equation (2.28) at 10 Hz is identified near $k_x \approx \pm 1.8$ rad/m. This means that the pole of the coupled wavenumber occurs at a larger wavenumber due to the influence of the plate, and this is mainly related to the mass effect provided by the plate.

The mass and damping effects of the third term in equation (2.28) can be simply compared by considering either the real part or the imaginary part of the third term separately. Figure 7 shows these results. It can be seen that the mass effect shifts the peak to a wavenumber above k_b and the effective damping due to the plate reduces the peak amplitude and broadens the peaks.

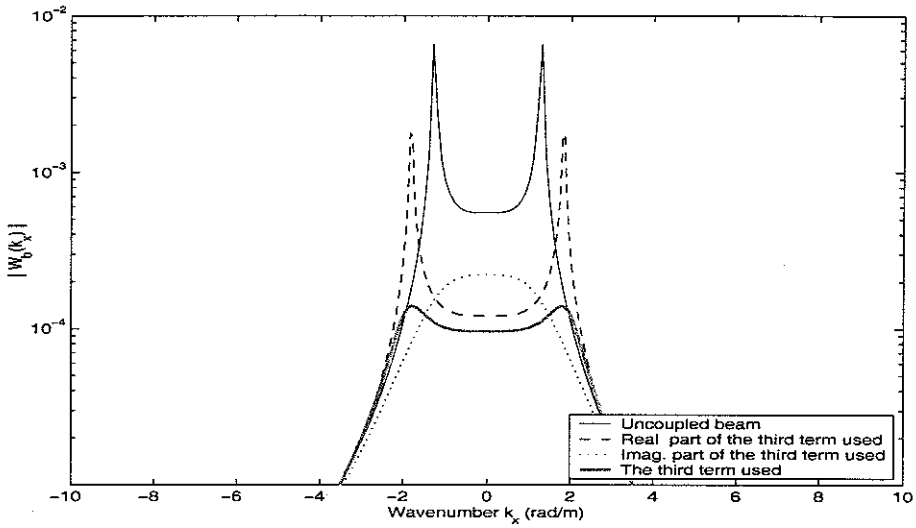

Figure 7. The effect of the complex third term in the denominator of equation (2.28) at 10 Hz in the wavenumber domain.

Figure 8 shows the transformed displacement response at 1 kHz. The pole occurs at $k_x \approx \pm 13.6$ rad/m which is closer to the corresponding uncoupled value of $k_b = 12.8$ rad/m. That is, the relative difference between the values of k_b and k_x is smaller at 1 kHz than at 10 Hz. As explained before, this is because the mass effect of the plate is reduced as frequency increases due to the k_p term. This can be confirmed by comparing the values of $\mu = m_p'' / \left(m_b' k_p \right)$, which changes from 3.5 at 10 Hz to 0.35 at 1 kHz.

Note that, because the uncoupled beam wavenumber k_b depends on frequency, to obtain the correct response of $\tilde{w}_b$, the wavenumber range of $\tilde{W}_b(k_x)$ to be considered should be changed according to the frequency. This means that $\tilde{W}_b(k_x)$ is not only a function of k_x but also of k_b as seen in Figures 6 and 8. Therefore, it is necessary to consider the response from the point of view of both k_x and k_b. By introducing the non-dimensional wavenumber $\gamma = k_x / k_b$ as before, the relationship between the response and k_x and $\tilde{k}_b$ can be examined.

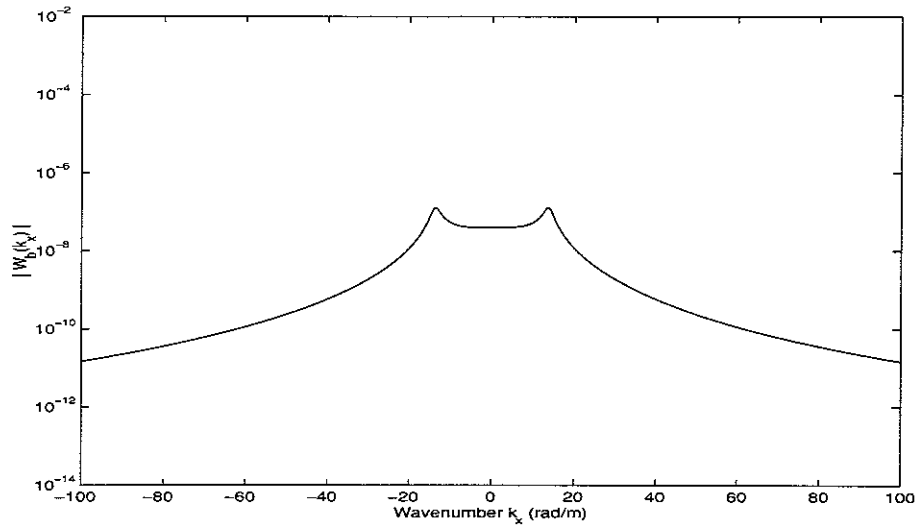

Figure 8. Fourier transformed displacement of the coupled infinite beam and plate as in Figure 1 at 1 kHz. $k_b = 12.8$ rad/m. $m_p'' / \left(m_b' k_p \right) = 0.35$.

Firstly, the relationship between the response $\tilde{W}_b(k_x)$ and the non-dimensional wavenumber is shown on linear axes in Figure 9. Because the response $\tilde{w}_b$ is obtained from the Fourier integral of $\tilde{W}_b(k_x)$, it can be seen that the most significant contribution of $\tilde{W}_b(k_x)$ to the responses is between $\gamma = -10$ and $+10$. However, to choose an appropriate response range, it seems reasonable to use a more consistent rule.

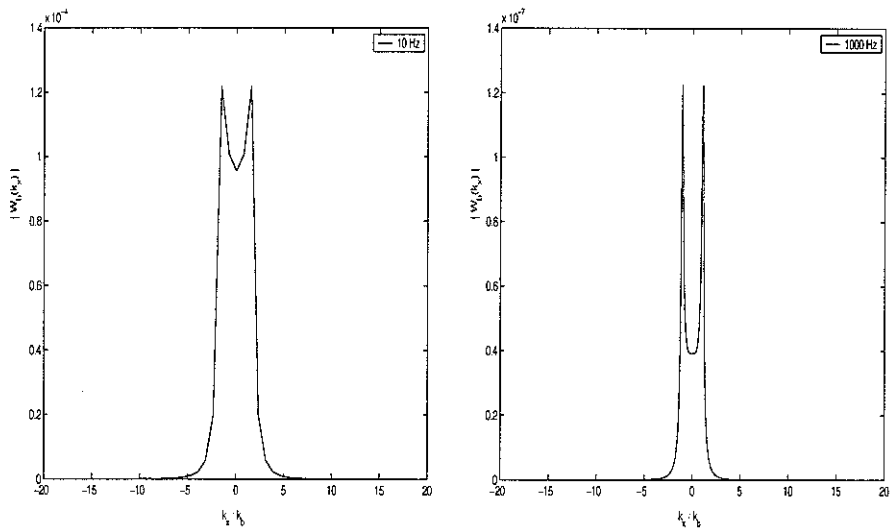

Figure 9. Fourier transformed displacement of the coupled infinite beam and plate as in Figure 1 at 10 Hz and 1 kHz.

One possible method is to truncate the range of integration by identifying a sufficiently low level response with respect to the maximum response. In such a case, a logarithmically scaled response would be more convenient than the linearly plotted response. The corresponding results are shown in Figure 10. From Figure 10, if the non-dimensional wavenumber range is chosen such that the difference of the Fourier transformed response remains less than 60 dB with respect to the maximum response, this would seem to be a reasonable range to estimate the most significant contribution to the response of $\tilde{W}_b(k_x)$ (see also Figure 9).

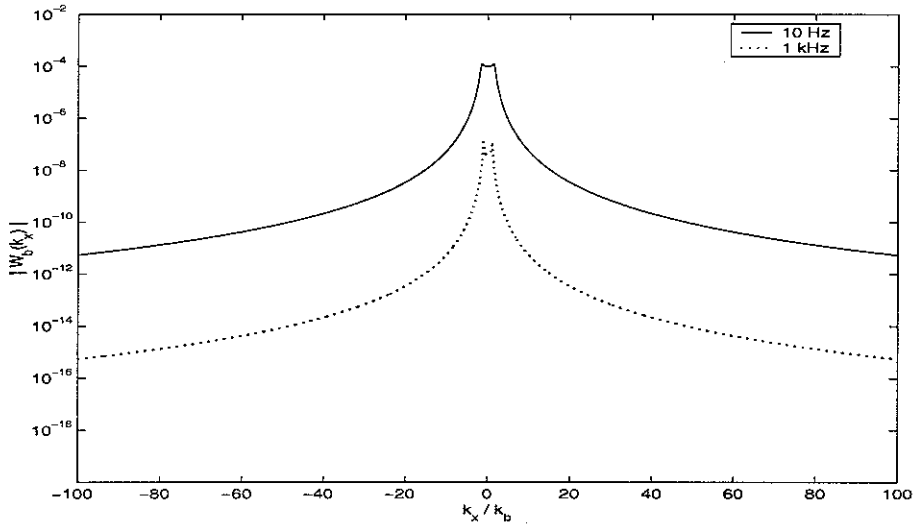

Figure 10. Fourier transformed displacement of the coupled infinite beam and plate as in Figure 1 with non-dimensional wavenumber at 10 Hz and 1 kHz.

The corresponding non-dimensional wavenumber range is approximately ±50 at 10 Hz and ±30 at 1 kHz. Therefore, the non-dimensional wavenumbers between ±50 are chosen for the whole frequency range being considered here (10 ~ 1000 Hz).

2.3.4 Coupled beam: Fourier transform

To confirm whether the range of non-dimensional wavenumber chosen is appropriate, the drive point response amplitude is compared in Figure 11. The results are obtained based on equation (2.36), which is derived using different ranges of the wavenumber k_x in the inverse Fourier transform. The function QUADL was used as previously for the evaluation of the integral. This indicates that the response amplitude is predicted reliably for a small range of non-dimensional wavenumber.

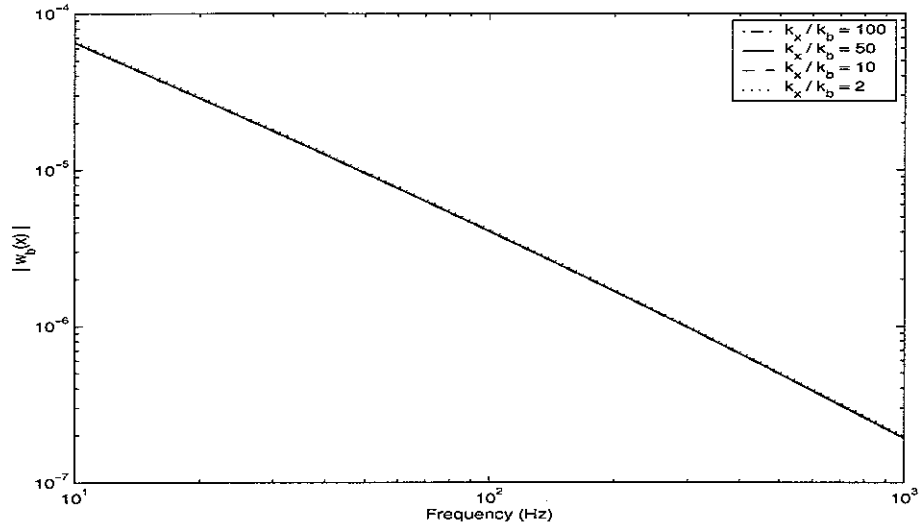

Figure 11. Displacement of the coupled infinite beam and plate as in Figure 1 at the excitation point when different ranges of non-dimensional wavenumber γ are considered.

When the non-dimensional wavenumber range for γ is between ± 2 the response is already close (error of 2.9 % at 10 Hz) to that for the case when $\gamma = \pm 100$ is used. Although it seems that there are no significant differences between the cases when $\gamma = \pm 10$ (error of 0.02 %), ± 50 (error of 0.0001 %) and ± 100, considering the percentage error with respect to the case when $\gamma = \pm 100$, the non-dimensional wavenumber range -50 to $+50$ seems to be reasonable in order to obtain an accurate response.

Assuming that the displacement of the coupled infinite beam based on the non-dimensional wavenumber range -50 to $+50$ is exact (Figure 10), the response errors arising from the choice of different integration ranges are compared here. Remembering that the range -50 to $+50$ is chosen based on the difference of 60 dB from the maximum response, it seems convenient to use the differences of 50 dB, 40 dB, 30 dB and 20 dB so that the non-dimensional wavenumber range to be considered can be changed according to Figure 10. The corresponding non-dimensional wavenumber ranges are -27 to $+27$, -15 to $+15$, -8 to $+8$ and -5 to $+5$ respectively. The errors with respect to the exact value are compared in Figure 12 for three different frequencies, 10 Hz, 100 Hz, and 1 kHz. Clearly, it can be seen that the differences are reduced with increasing range. Although a greater range results in smaller errors, it also requires much more computation time. Therefore, the non-dimensional wavenumber ranges (or dB) may be reconsidered to reduce the computation time as even a difference of 20 dB (non-dimensional wavenumber -5 to $+5$) results in a maximum error of less than 0.25 %.

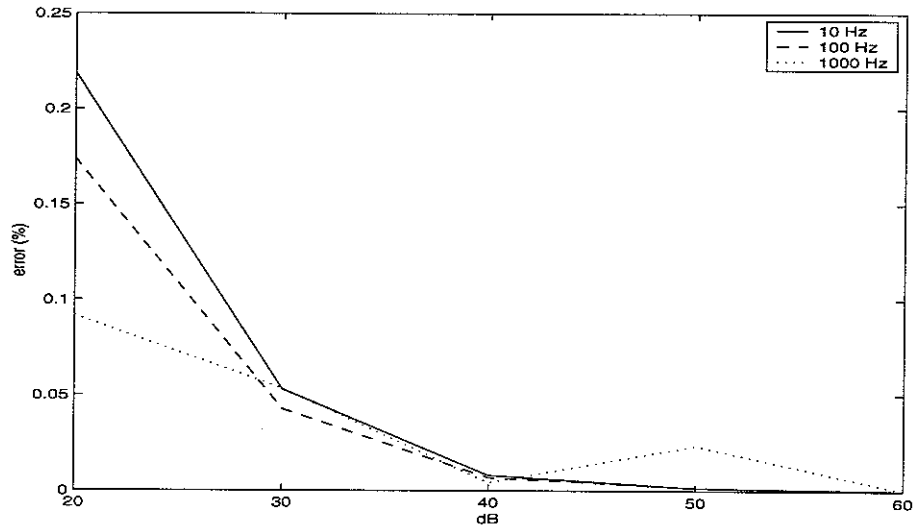

Figure 12. The errors of the displacement due to the differences with respect to the maximum level of the Fourier transformed displacement shown in Figure 10 (The result based on 60 dB difference is assumed to be the exact value).

Instead of adaptive quadrature, the Fast Fourier Transform (FFT) can be used to evaluate $\tilde{w}_b(x)$. The advantage of the FFT is that results can be obtained more rapidly than using an adaptive quadrature. However, consideration should be given to the data resolution of $\tilde{W}_b(k_x)$. As seen in Figure 9, if $\tilde{W}_b(k_x)$ is not calculated with sufficient resolution in terms of k_x, then some important data can be lost, particularly at the peaks, and this results in inaccurate predictions. The relationship between the data resolution of $\tilde{W}_b(k_x)$ and the response $\tilde{w}_b(x)$ has therefore been studied.

Data resolution Δk_x in the FFT defines the response ranges of $\tilde{w}_b(x)$ as follows [8].

$$x_{\max} = \frac{2\pi}{\Delta k_x}. \tag{2.44}$$

In fact, because the results calculated based on the FFT show symmetric responses, only half of the inverse Fourier transforms are shown and their limit can be defined by

$$x_{fold} = \frac{x_{\max}}{2}. \tag{2.45}$$

Using the symmetric Fourier transformed displacement such as that shown in Figure 10, the whole FFT data was obtained. Figures 13 and 14 present these results, which show the real part of the displacement of the coupled beam as a function of coordinate position x. For

both cases, the same non-dimensional wavenumber range $\gamma = -50$ to +50 is used. Because the same resolution of non-dimensional wavenumber is used, the resolution of the wavenumber Δk_x is effectively adjusted based on k_b. In this case the number of values of wavenumber k_x used is 2561, independent of frequency.

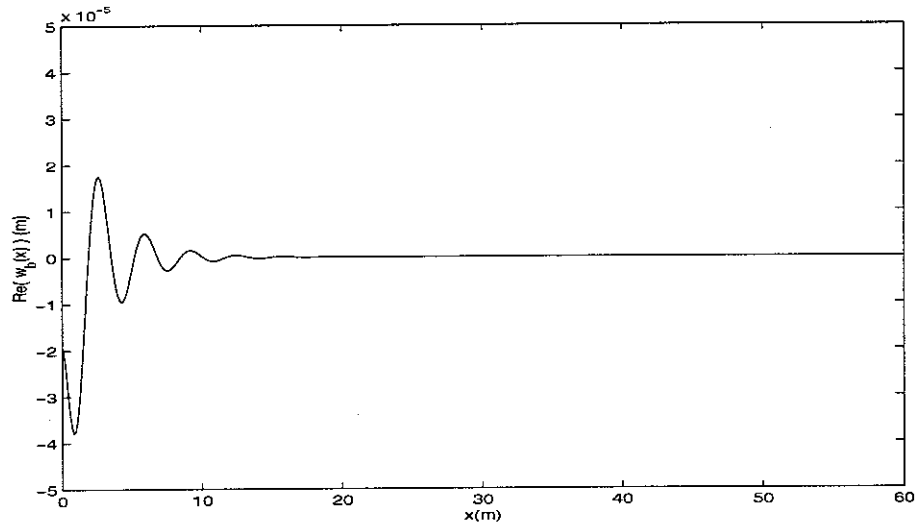

Figure 13. Real part of displacement of the coupled infinite beam as in Figure 1 at 10 Hz. Non-dimensional wavenumber range used is $\gamma = -50$ to +50, $k_x = -64$ to +64, $\Delta k_x = 0.05$, $x_{fold} = 62.8\,\mathrm{m}$, $m_p''/\left(m_b' k_p\right) = 3.5$.

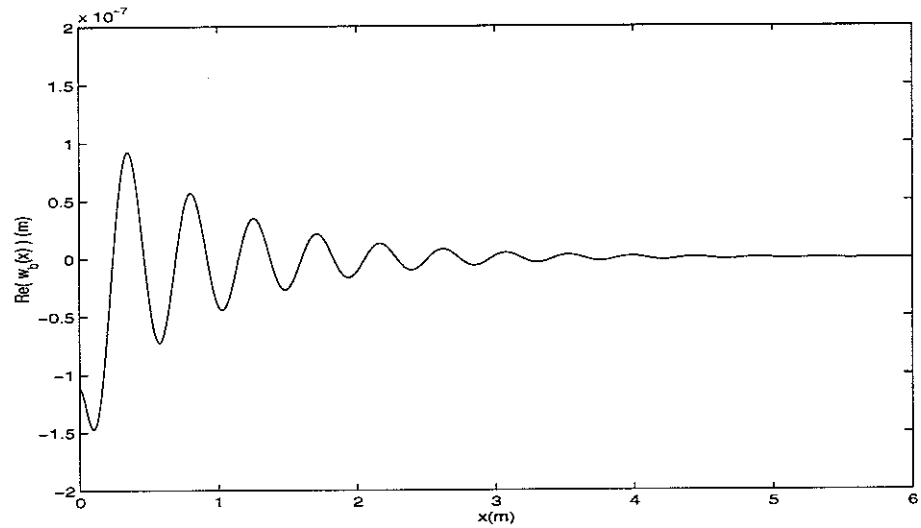

Figure 14. Real part of displacement of the coupled infinite beam as in Figure 1 at 1 kHz. Non-dimensional wavenumber range used is $\gamma = -50$ to +50, $k_x = -640$ to +640, $\Delta k_x = 0.5$, $x_{fold} = 6.28\,\mathrm{m}$, $m_p''/\left(m_b' k_p\right) = 0.35$.

In both figures it can be seen that the response decays to a negligible level within the range limited by x_{fold}. Therefore, the chosen value of Δk_x based on the non-dimensional wavenumber seems to be reasonable for obtaining the correct response.

Note that the displacement at 10 Hz decays in a smaller number of cycles than the 1 kHz case. As mentioned above, this is also related the effect of the plate. Because the value of $\mu = m_p'' / \left(m_b' k_p \right)$ at 10 Hz is larger than that at 1 kHz, the effective damping due to the plate is greater at 10 Hz than at 1 kHz. Accordingly, the response of the beam at 10 Hz decays in fewer cycles.

As equation (2.36) describes the motion of the infinite coupled beam, it is expected that the displacement amplitude of the beam in the vicinity of the excitation point $x = 0$ has no rotation. This result is identified in Figure 15. The dashed line in the figure represents the amplitude of the displacement. The other two curves, the real and imaginary parts, correspond to the displaced shape at two different times. It can be seen that the slope in each case equals zero at $x = 0$. The response at $x < 0$ is symmetric in shape with respect to the axis $x = 0$.

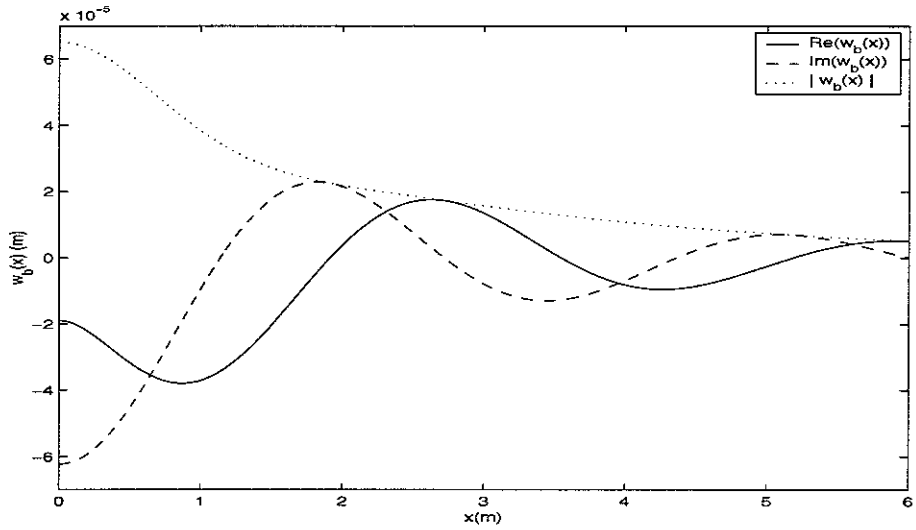

Figure 15. Displacement of the coupled infinite beam as in Figure 1 at 10 Hz. Non-dimensional wavenumber range used is $\gamma = -50$ to $+50$, $k_x = -64$ to $+64$, $\Delta k_x = 0.05$, $x_{fold} = 62.8\,\mathrm{m}$, $m_p'' / \left(m_b' k_p \right) = 3.5$.

The response based on the discrete FFT is compared in Figure 16 with that calculated by the Fourier transform method, for which QUADL is used. Because a unit point force is applied, the velocity response represents the mobility of the structure. Figure 16 shows good

agreement between the point mobilities of the infinite beam coupled to the semi-infinite plate obtained from the two methods (0.2 % difference).

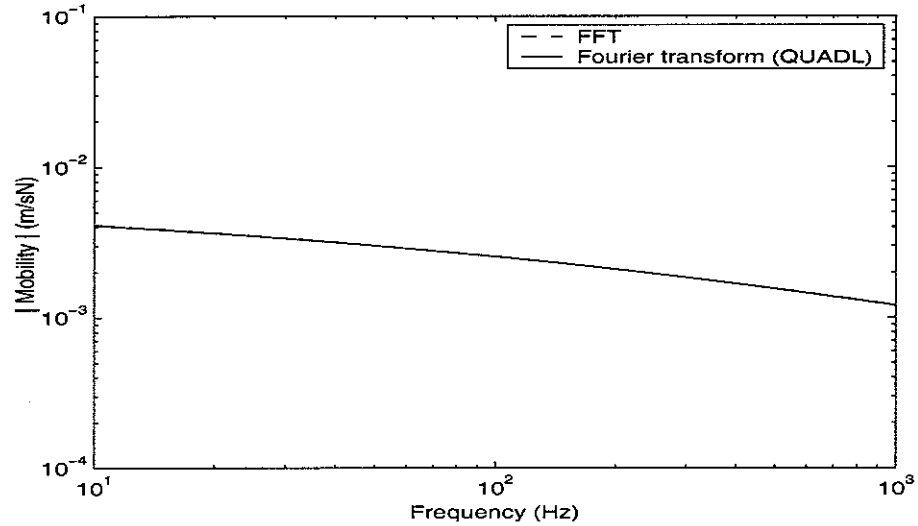

Figure 16. Comparison of the point mobility of the infinite beam and plate calculated by the Fourier transform method and the FFT. Non-dimensional wavenumber range $\gamma = -50$ to $+50$ is considered in the Fourier transform.

Finally, the response calculated by the Fourier transform method is compared with the results of the previously developed wave method [1]. Figure 17 shows the point mobilities, calculated by the different methods. The results show good agreement as well (2.5 % difference).

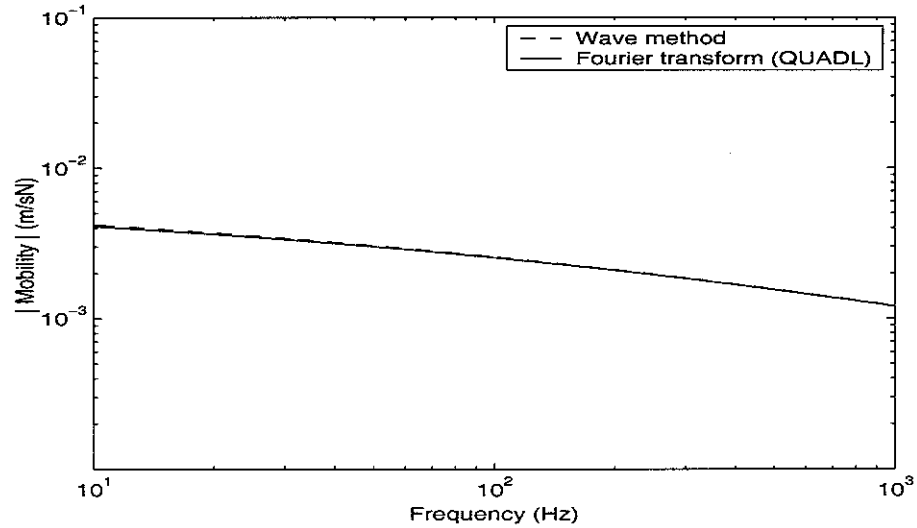

Figure 17. Comparison of the point mobility of the infinite beam and plate calculated by the Fourier transform method and wave method. Non-dimensional wavenumber range $\gamma = -50$ to $+50$ is considered in the Fourier transform.

3. INFINITE BEAM COUPLED TO FINITE WIDTH PLATE: BEAM-EXCITED

3.1 Structural coupling

In this section, a built-up structure is considered consisting of an infinite beam and a plate of finite width as shown in Figure 18. A pinned boundary condition is considered at the plate along the opposite edge parallel to the beam.

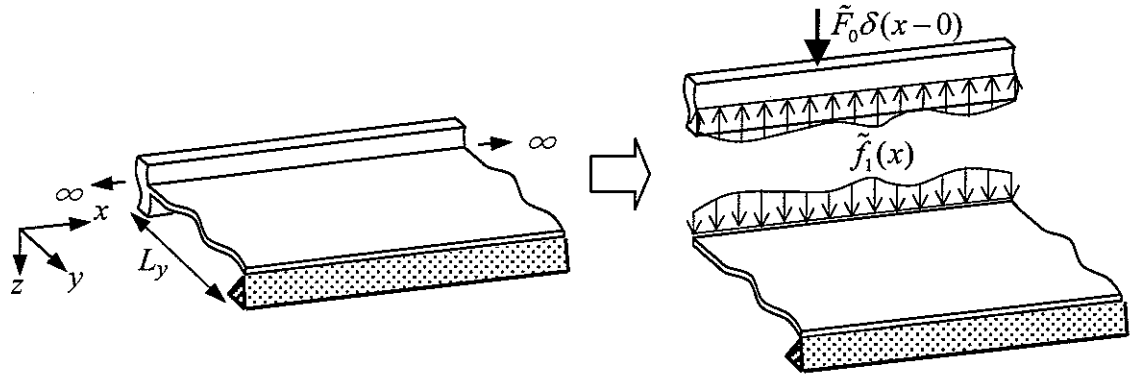

Figure 18. A built-up structure consisting of an infinite beam attached to a finite width plate.

Including the reflected travelling wave and nearfield wave generated at the opposite edge of the finite plate, equation (2.15) can be extended as follows.

$$\tilde{W}_p(k_x,y)=\tilde{B}e^{\tilde{k}_{y1}y}+\tilde{C}e^{\tilde{k}_{y2}y}+\tilde{\beta}_{y1}\tilde{r}\tilde{B}e^{-\tilde{k}_{y1}y}+\tilde{D}e^{-\tilde{k}_{y2}y} \tag{3.1}$$

where $\tilde{\beta}_{y1}=e^{\tilde{k}_{y1}2L_y}$ is the propagating wave attenuation coefficient of the plate, which represents attenuation as well as phase shift over the length $2L_y$, $\tilde{r}$ is the complex reflection coefficient at the edge of the plate $y=L_y$ and $\tilde{D}$ is the amplitude of the near field wave which is generated at the opposite edge of the plate.

All boundary conditions between the plate and beam are assumed to be the same as presented in the previous section. From boundary condition (i),

$$\tilde{W}_b(k_x)=\tilde{W}_p(k_x,y)\Big|_{y=0}=\left(\tilde{B}+\tilde{C}+\tilde{\beta}_{y1}\tilde{r}\tilde{B}+\tilde{D}\right). \tag{3.2}$$

From boundary condition (ii),

$$\left.\frac{\partial\tilde{W}_p(k_x,y)}{\partial y}\right|_{y=0}=\left(1-\tilde{\beta}_{y1}\tilde{r}\right)\tilde{k}_{y1}\tilde{B}+\tilde{k}_{y2}\tilde{C}-\tilde{k}_{y2}\tilde{D}=0, \tag{3.3}$$

and from the force equilibrium condition,

$$\tilde{F}_1(k_x) = \tilde{D}_p \left[\frac{\partial^3 \tilde{W}_p(k_x, y)}{\partial y^3} \right]_{y=0} = \tilde{D}_p \left[\tilde{k}_{y1}^3 \left(1 - \tilde{\beta}_{y1} \tilde{r}\right) \tilde{B} + \tilde{k}_{y2}^3 \tilde{C} - \tilde{k}_{y2}^3 \tilde{D} \right]. \tag{3.4}$$

It is necessary to introduce one more boundary conditions because there are two more unknown variables $\tilde{D}$ and $\tilde{r}$.

(iv) Pinned condition at the opposite edge of the plate at $y = L_y$,

$$\tilde{W}_p(k_x, y)\Big|_{y=L_y} = \left(e^{\tilde{k}_{y1} L_y} + \tilde{\beta}_{y1} \tilde{r} e^{-\tilde{k}_{y1} L_y} \right) \tilde{B} + e^{\tilde{k}_{y2} L_y} \tilde{C} + e^{-\tilde{k}_{y2} L_y} \tilde{D} = 0. \tag{3.5}$$

The pinned condition also yields $\tilde{r} = -1$, from which $e^{\tilde{k}_{y1} L_y} + \tilde{\beta}_{y1} \tilde{r} e^{-\tilde{k}_{y1} L_y} = 0$. Thus equation (3.5) can be expressed in the simpler form

$$\tilde{W}_p(k_x, y)\Big|_{y=L_y} = e^{\tilde{k}_{y2} L_y} \tilde{C} + e^{-\tilde{k}_{y2} L_y} \tilde{D} = 0.$$

Therefore,

$$\tilde{D} = -e^{2\tilde{k}_{y2} L_y} \tilde{C} = -\tilde{\beta}_{y2} \tilde{C}. \tag{3.6}$$

Substituting equation (3.6) into equation (3.3), the relationship between $\tilde{B}$ and $\tilde{C}$ is defined.

$$\tilde{C} = -\frac{\tilde{k}_{y1} \left(1 + \tilde{\beta}_{y1}\right)}{\tilde{k}_{y2} \left(1 + \tilde{\beta}_{y2}\right)} \tilde{B}. \tag{3.7}$$

Therefore, from equations (3.6) and (3.7), equation (3.2) becomes

$$\tilde{W}_b(k_x) = \frac{-\tilde{k}_{y1} \left(1 + \tilde{\beta}_{y1}\right)\left(1 - \tilde{\beta}_{y2}\right) + \tilde{k}_{y2} \left(1 - \tilde{\beta}_{y1}\right)\left(1 + \tilde{\beta}_{y2}\right)}{\tilde{k}_{y2} \left(1 + \tilde{\beta}_{y2}\right)} \tilde{B}. \tag{3.8}$$

From equations (3.6), (3.7) and (3.8), the equation for force equilibrium condition is expressed as

$$\begin{aligned}
\tilde{F}_1(k_x) &= \tilde{D}_p \left[\tilde{k}_{y1}^3 \left(1 + \tilde{\beta}_{y1}\right) \tilde{B} + \tilde{k}_{y2}^3 \left(1 + \tilde{\beta}_{y2}\right) \tilde{C} \right]. \\
&= \tilde{D}_p \tilde{k}_{y1} \left(1 + \tilde{\beta}_{y1}\right) \left(\tilde{k}_{y1}^2 - \tilde{k}_{y2}^2 \right) \tilde{B} \\
&= \tilde{D}_p \frac{\tilde{k}_{y1} \tilde{k}_{y2} \left(\tilde{k}_{y1}^2 - \tilde{k}_{y2}^2 \right)}{-\tilde{k}_{y1} \left(1 - \tilde{\beta}_{y2}\right) / \left(1 + \tilde{\beta}_{y2}\right) + \tilde{k}_{y2} \left(1 - \tilde{\beta}_{y1}\right) / \left(1 + \tilde{\beta}_{y1}\right)} \tilde{W}_b(k_x).
\end{aligned} \tag{3.9}$$

As $\left(1-\tilde{\beta}_{y2}\right)/\left(1+\tilde{\beta}_{y2}\right)=-\tanh\left(\tilde{k}_{y2}L_y\right)$ and $\left(1-\tilde{\beta}_{y1}\right)/\left(1+\tilde{\beta}_{y1}\right)=-\tanh\left(\tilde{k}_{y1}L_y\right)$, equation (3.9) can be expressed more simply as

$$\tilde{F}_1(k_x)=\tilde{D}_p\frac{\tilde{k}_{y1}\tilde{k}_{y2}\left(\tilde{k}_{y1}^2-\tilde{k}_{y2}^2\right)}{\tilde{k}_{y1}\tanh\left(\tilde{k}_{y2}L_y\right)-\tilde{k}_{y2}\tanh\left(\tilde{k}_{y1}L_y\right)}\tilde{W}_b(k_x). \tag{3.10}$$

Therefore, the impedance per unit length for the finite plate becomes

$$\tilde{Z}'_p(k_x)=\frac{\tilde{D}_p}{i\omega}\frac{\tilde{k}_{y1}\tilde{k}_{y2}\left(\tilde{k}_{y1}^2-\tilde{k}_{y2}^2\right)}{\tilde{k}_{y1}\tanh\left(\tilde{k}_{y2}L_y\right)-\tilde{k}_{y2}\tanh\left(\tilde{k}_{y1}L_y\right)}. \tag{3.11}$$

Finally substituting for the reaction force of the finite width plate $\tilde{F}_1(k_x)$ into equation (2.6), for the coupled structure shown in Figure 18, one has the transformed beam response

$$\tilde{W}_b(k_x)=\frac{\tilde{F}_0}{\tilde{D}_b k_x^4-m'_b\omega^2+\tilde{H}(k_x)} \tag{3.12}$$

where $\tilde{H}(k_x)$ is defined as

$$\tilde{H}(k_x)=\tilde{D}_p\frac{\tilde{k}_{y1}\tilde{k}_{y2}\left(\tilde{k}_{y1}^2-\tilde{k}_{y2}^2\right)}{\tilde{k}_{y1}\tanh\left(\tilde{k}_{y2}L_y\right)-\tilde{k}_{y2}\tanh\left(\tilde{k}_{y1}L_y\right)}. \tag{3.13}$$

3.2 Numerical analysis

Numerical simulation is carried out using equation (3.12) for the coupled structure as in Figure 18.

For comparison with the numerical results, FEM is used. Previously [1, 3] the beam in the FEM was modelled by membrane elements which will allow shear strains and rotary inertia effects of the cross-section of the beam [9]. However, in the present analytical model, the response of the beam is calculated based on Euler-Bernoulli beam theory that does not consider the rotary inertia effect and shear deformation. Accordingly some difference in responses can occur, particularly at high frequencies. Therefore, in the present report, beam elements following the Euler-Bernoulli beam theory are used in the FE models instead of the membrane elements.

The opposite edge of the plate, parallel to the beam, is considered to be pinned and the neutral axis of the beam is assumed to lie in the centre of the beam as in the previous section. Most dimensions of the FE model are the same as those presented in Table 1. However, to approximate and compare with the semi-infinite beam structure, a long beam of length 8.0 m

is modelled. Accordingly the length of the plate also becomes 8.0 m. One end of the beam at $x = 0$, where the external force is applied, and the corresponding plate edge, are assumed to be sliding to represent symmetry. The other end and the corresponding plate edge are assumed to be free. To simulate an anechoic termination of the free end, structural damping of between 0.05 and 0.65 is added gradually in both the beam and plate along the final 2.0 m length.

As explained in section 2.3, the numerical response based on the Fourier transform method is symmetric in shape with respect to $x = 0$. Therefore, the point mobility of the FE model with the sliding condition is twice that of the fully infinite structure, as the sliding condition requires symmetry and accordingly, only half the force is necessary for the half model. These point mobilities are compared in Figure 19.

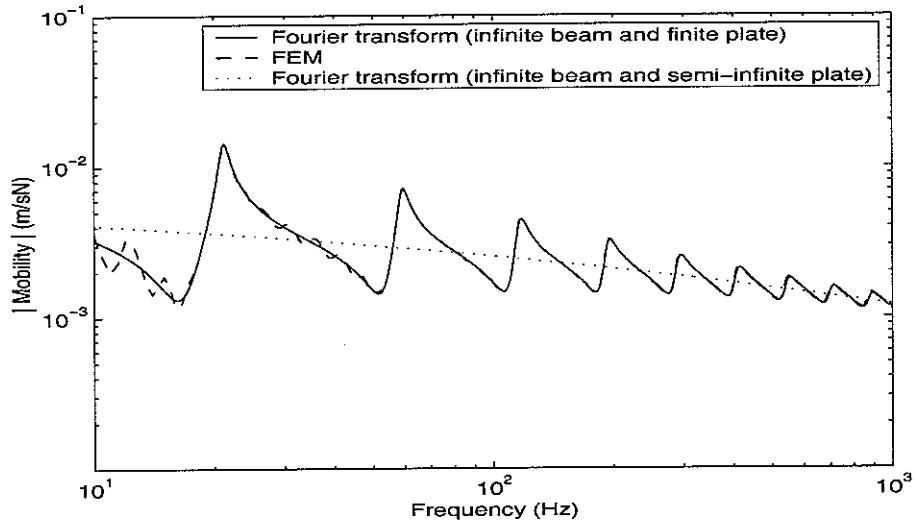

Figure 19. Comparison of the point mobility calculated by Fourier transform and FEM for the infinite beam and finite width plate as in Figure 18. Values of $\gamma = -50$ to $+50$ are considered in the inverse Fourier transform.

Some low frequency fluctuations occur in the FEM result. Although an attempt was made to simulate an infinite length using high structural damping near the free end, the FE model is actually finite and the global modes are related to the finite structure. Nevertheless, as expected, good agreement is found in the mid and high frequency region. Note that because the beam is assumed to be infinite in the Fourier transform method, the peaks and dips of the mobility are only related to dynamic characteristics of the finite width plate. The result in Figure 19 can be seen to oscillate around that of the infinite beam and semi-infinite plate (from Figure 16).

4. FINITE BEAM COUPLED TO FINITE PLATE: BEAM-EXCITED

4.1 Motion of finite beam by Fourier series

In the previous section, the motion of the infinite beam coupled to a finite width plate has been described and formulated. As this defines the relationship between the beam and the plate, the finite beam response can be obtained if that relationship is maintained.

Consider the coupled beam/plate system shown in Figure 20 with both ends of the beam in a sliding condition. The plate edge parallel to the beam is considered to be pinned as before, and the other two edges are assumed to be sliding.

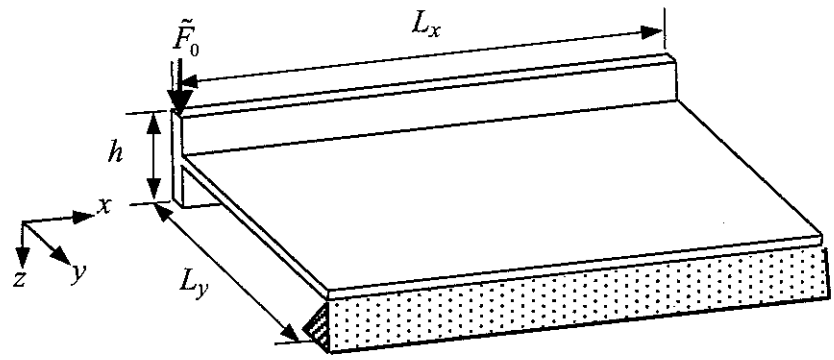

Figure 20. A built-up structure consisting of a finite beam attached to a finite plate with a pinned opposite edge.

Then the behaviour of the coupled beam with sliding conditions at its ends can be expressed in terms of cosine orders as follows.

$$\cos\left(\frac{n\pi x}{L_x}\right),\ n=0,1,2,3,\cdots \tag{4.1}$$

where L_x is the length of the coupled beam, n is the number of half-cosine waves along the coupled beam. Equation (4.1) can be simplified as

$$\cos\left(k_{x,n}x\right),\ n=0,1,2,3,\cdots. \tag{4.2}$$

where $k_{x,n}=n\pi/L_x$. Note that the relationship between the coupled beam and the plate defined in the previous sections is maintained. Thus, the motion of the finite coupled beam with sliding end conditions may be written as

$$\tilde{w}_b(x) = \frac{\tilde{W}_b(k_{x,0})}{2} + \sum_{n=1}^{\infty} \tilde{W}_b(k_{x,n}) \cos(k_{x,n} x), \tag{4.3}$$

or simply

$$\tilde{w}_b(x) = \frac{\tilde{W}_{b,0}}{2} + \sum_{n=1}^{\infty} \tilde{W}_{b,n} \cos(k_{x,n} x) \tag{4.4}$$

where $\tilde{W}_{b,n} = \tilde{W}_b(k_{x,n})$ is the n^{th} component of the motion of the coupled beam, which is defined in equation (2.28) for the semi-infinite plate case and equation (3.12) for the finite width plate case. $\tilde{W}_{b,0}/2$ is considered as the value for rigid motion of the beam ($k_x = 0$). Consequently, the motion of the coupled beam is expressed as a Fourier series possessing only cosine functions.

In the same manner, the motion of the plate shown in Figure 20 at each position y can also be written in terms of the Fourier series as follows.

$$\tilde{w}_p(x, y) = \frac{\tilde{W}_{p,0}(y)}{2} + \sum_{n=1}^{\infty} \tilde{W}_{p,n}(y) \cos(k_{x,n} x) \tag{4.5}$$

where $\tilde{W}_{p,n}(y) = \tilde{W}_p(k_{x,n}, y)$ is the n^{th} component of the motion of the plate, which is presented in equation (3.1). Thus the method of the previous section can be used, replacing the Fourier transform by a Fourier series.

4.2 Power balance

In previous analysis using the wave method [1], the power relationship for the same structure was presented based on the wave method, where it was shown that the power balance for the plate was not maintained. This was one of the reasons why another method such as the Fourier transform method was developed in addition to the wave method. By the same procedure of power comparison, it is shown here that the Fourier transform method can accurately predict the power relationship between subsystems of the coupled structure.

The power balance for the coupled structure shown in Figure 20 is presented schematically in Figure 21. P_{input} means the total power input, $P_{b \to p}$ means the net power transferred from the beam to the plate, $P_{b,dis}$ means the power dissipated in the beam and $P_{p,dis}$ represents the power dissipated in the plate.

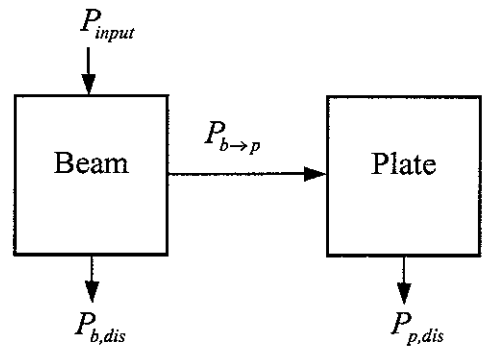

Figure 21. Power balance between subsystems of the coupled structure as in Figure 20.

The total power injected into the coupled beam-plate structure by the point force applied at $x = 0$ is given by

$$P_{total} = \frac{1}{2}\mathrm{Re}\left\{ \tilde{F}_0^* \ \tilde{v}_0 \right\} \tag{4.6}$$

$$\text{or } P_{total} = \frac{1}{2}\mathrm{Re}\left\{ \tilde{F}_0^* \tilde{w}_0 i\omega \right\} \tag{4.7}$$

where $\tilde{w}_0 = \tilde{w}_b(x)\big|_{x=0}$ can be obtained from equation (4.4) and * indicates complex conjugate.

The Fourier series for the force acting on the plate of the coupled structure shown in Figure 20 is

$$\tilde{f}_1(x) = \frac{\tilde{F}_{1,0}}{2} + \sum_{n=1}^{\infty} \tilde{F}_{1,n} \cos(k_{x,n} x), \tag{4.8}$$

where the Fourier transformed force $\tilde{F}_{1,n} = \tilde{F}_1(k_{x,n})$ is defined from equation (3.10) where $k_{x,n} = n\pi / L_x$. Therefore, the net power transferred from the beam to the plate can be expressed in terms of the distributed interaction force and responses.

$$P_{b\to p} = \frac{1}{2}\int_0^{L_x} \mathrm{Re}\left\{ \tilde{f}(x)^* \tilde{v}_b(x) \right\} dx, \tag{4.9}$$

where $\tilde{v}_b(x) = i\omega \tilde{w}_b(x)$ is the velocity response of the coupled beam and L_x is the length of the beam.

As before [1], the dissipated power is obtained from the strain energy of the corresponding substructure, noting that this differs from the kinetic energy as the beam

structure does not have many vibrational modes in the frequency band of interest. Also, although the plate is expected to have more modes, it shows beam-like behaviour in the y direction [3]. Therefore, for obtaining the dissipated power of the plate, it also seems appropriate to use the strain energy of the plate. As will be shown, using this assumption the results show good agreement.

The dissipated power in the finite beam can be written as [10]

$$P_{b,dis} = \omega \eta_b E_b . \tag{4.10}$$

where E_b is the maximum strain energy in a cycle in the beam, given by

$$E_b = \frac{D_b}{2} \int_0^{L_x} \left| \frac{d^2 \tilde{w}_b(x)}{dx^2} \right|^2 dx . \tag{4.11}$$

The second derivative of $\tilde{w}_b(x)$ can be obtained in terms of the Fourier series as

$$\frac{d^2 \tilde{w}_b(x)}{dx^2} = -\sum_{n=1}^{\infty} k_{x,n}^2 \tilde{W}_{b,n} \cos(k_{x,n} x) \tag{4.12}$$

where $\tilde{W}_{b,n} = \tilde{W}_b(k_{x,n})$.

The strain energy in a plate is given by [11]

$$E_{p,strain} = \frac{D_p}{2} \int_0^{L_x} \int_0^{L_y} \left[\left(\frac{\partial^2 w_p}{\partial x^2} \right)^2 + \left(\frac{\partial^2 w_p}{\partial y^2} \right)^2 + 2\nu \frac{\partial^2 w_p}{\partial x^2} \frac{\partial^2 w_p}{\partial y^2} + 2(1-\nu) \left(\frac{\partial^2 w_p}{\partial x \partial y} \right)^2 \right] dy dx \tag{4.13}$$

where $w_p = w_p(x, y, t)$ is time dependent and therefore, each term in the strain energy can be regarded as a time dependent term. Assuming that each term is either in or out of phase the maximum strain energy in a cycle can be obtained from twice the time-averaged value of each term of equation (4.13), and the maximum strain energy will be presented as [12]

$$E_{p,strain} = \frac{D_p}{2} \int_0^{L_x} \int_0^{L_y} \left[\left| \frac{\partial^2 \tilde{w}_p}{\partial x^2} \right|^2 + \left| \frac{\partial^2 \tilde{w}_p}{\partial y^2} \right|^2 + 2\nu \, \mathrm{Re} \left\{ \left(\frac{\partial^2 \tilde{w}_p}{\partial x^2} \right) \left(\frac{\partial^2 \tilde{w}_p}{\partial y^2} \right)^* \right\} + 2(1-\nu) \left| \frac{\partial^2 \tilde{w}_p}{\partial x \partial y} \right|^2 \right] dy dx \tag{4.14}$$

where $\tilde{w}_p = \tilde{w}_p(x, y)$. As the motion of the finite plate $\tilde{w}_p$ is given by equation (4.5), the second derivative of $\tilde{w}_p$ with respect to the variables x and y can be expressed using the Fourier series. The second derivative of $\tilde{w}_p$ with respect to x is

$$\frac{\partial^2 \tilde{w}_p}{\partial x^2} = -\sum_{n=1}^{\infty} k_{x,n}^2 \tilde{W}_{p,n} \cos(k_{x,n} x). \tag{4.15}$$

The second derivative of $\tilde{W}_{p,n}$ with respect to y is

$$\frac{\partial^2 \tilde{W}_{p,n}}{\partial y^2} = \left(\tilde{B}\tilde{k}_{y1}^2 e^{\tilde{k}_{y1} y} + \tilde{C}\tilde{k}_{y2}^2 e^{\tilde{k}_{y2} y} + \tilde{\beta}_{y1}\tilde{r}\tilde{k}_{y1}^2 \tilde{B} e^{-\tilde{k}_{y1} y} + \tilde{D}\tilde{k}_{y2}^2 e^{-\tilde{k}_{y2} y} \right). \tag{4.16}$$

and accordingly, the Fourier expression for the second derivative of $\tilde{w}_p$ with respect to y becomes

$$\frac{\partial^2 \tilde{w}_p}{\partial y^2} = \frac{1}{2}\frac{\partial^2 \tilde{W}_{p,0}}{\partial y^2} + \sum_{n=1}^{\infty} \frac{\partial^2 \tilde{W}_{p,n}}{\partial y^2} \cos(k_{x,n} x). \tag{4.17}$$

Also the derivative of $\tilde{W}_{p,n}$ with respect to y is

$$\frac{\partial \tilde{W}_{p,n}}{\partial y} = \left(\tilde{B}\tilde{k}_{y1} e^{\tilde{k}_{y1} y} + \tilde{C}\tilde{k}_{y2} e^{\tilde{k}_{y2} y} - \tilde{\beta}_{y1}\tilde{r}\tilde{k}_{y1} \tilde{B} e^{-\tilde{k}_{y1} y} - \tilde{D}\tilde{k}_{y2} e^{-\tilde{k}_{y2} y} \right). \tag{4.18}$$

Therefore, the second derivative of $\tilde{w}_p$ with respect to xy is

$$\frac{\partial^2 \tilde{w}_p}{\partial x \partial y} = -\sum_{n=1}^{\infty} k_{x,n} \frac{\partial \tilde{W}_{p,n}}{\partial y} \sin(k_{x,n} x). \tag{4.19}$$

Therefore, substituting equations (4.15), (4.17) and (4.19) in equation (4.14), the maximum strain energy can be obtained. Finally, the dissipated power in the finite plate is given by

$$P_{p,dis} = \omega \eta_p E_{p,strain}. \tag{4.20}$$

4.3 Numerical analysis

4.3.1 Response of the coupled structure

Numerical analysis has been performed for the coupled structure consisting of a finite beam attached to a finite plate shown in Figure 20. As in the earlier sections the second moment of area of the beam is calculated with its neutral axis lying in the centre of the beam as above and the dimensions of the structure are given in Table 2. The opposite edge parallel to the beam is considered pinned. Note that the behaviour of the plate is defined by the wavenumber k_x in the x direction. Thus, as both ends of the beam are considered sliding,

then these edges of the plate are also assumed as sliding, although at $y = L_y$ the plate is pinned.

Table 2. Dimensions of the built-up structure shown in Figure 20.

Material	Perspex	Plate width, L_y (m)	0.75
Young's modulus, E (GNm^{-2})	4.4	Thickness, t (mm)	5.9
Poisson's ratio, ν	0.38	Height of the beam, h (mm)	68.0
Density, ρ (kgm^{-3})	1152.0	Loss factor of the beam, η_b	0.05
Beam length, L_x (m)	2.0	Loss factor of the plate, η_p	0.05

For the case when the external, unit magnitude, point force $\tilde{F}_0$ is applied at $x = 0$, the point mobility is shown in Figure 22 obtained using FEM and the Fourier series method. In equation (4.4), $n = 400$ is used, which approximately corresponds to the wavenumber $k_x = 640$ rad/m at 1 kHz corresponding to the non-dimensional wavenumber $\gamma = 50$. The number of elements used in the FE model is 5016 when beam elements are used for the beam subsystem.

As seen in the figure below, the result obtained by the Fourier series method shows very good agreement with that of FEM. Note that the responses agree well even in the higher frequency region. As explained in section 3.2, this is because the beam in the FE model was modelled by beam elements, which follow the Euler-Bernoulli beam theory. If membrane elements are used for the beam as in [1], as the membrane element beam allows the shear deformation and rotary effect, the resonance frequencies obtained by the FEM are lower than those of analytical response using the Fourier series method. This can be confirmed if point mobilities of an uncoupled beam are compared. If an uncoupled beam of 2.0 m length and properties as in Table 2 is considered to compare the mobilities where both ends of the beam are considered to be sliding, the resonance frequencies show approximately 9 % difference at 700 Hz between an Euler-Bernoulli beam and the membrane element representation.

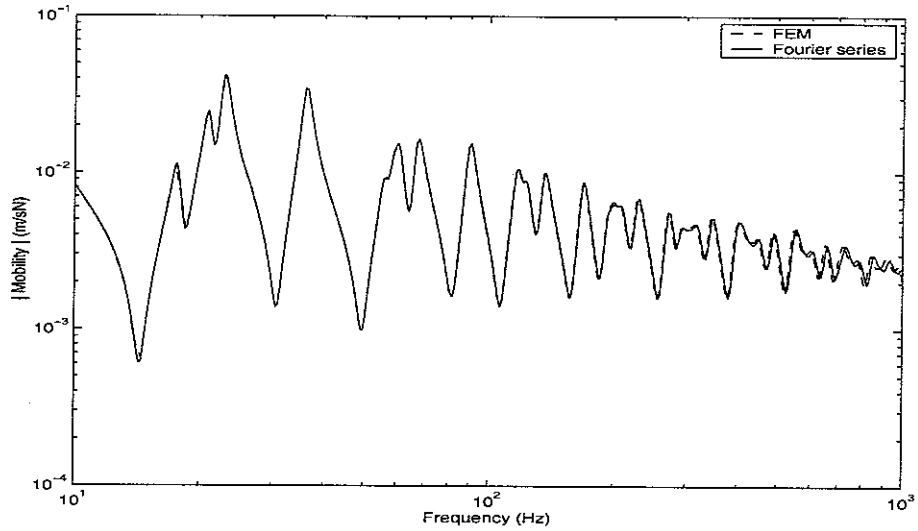

Figure 22. Comparison of the mobility calculated by different methods for the coupled finite beam/plate structure as in Figure 20 ($\eta_p = 0.05$ in the plate, $\eta_b = 0.05$ in the beam, point force applied at $x = 0$).

In addition to the point mobility comparison, an example of a transfer mobility to the plate is shown in Figure 23, which also shows good agreement with that of FEM.

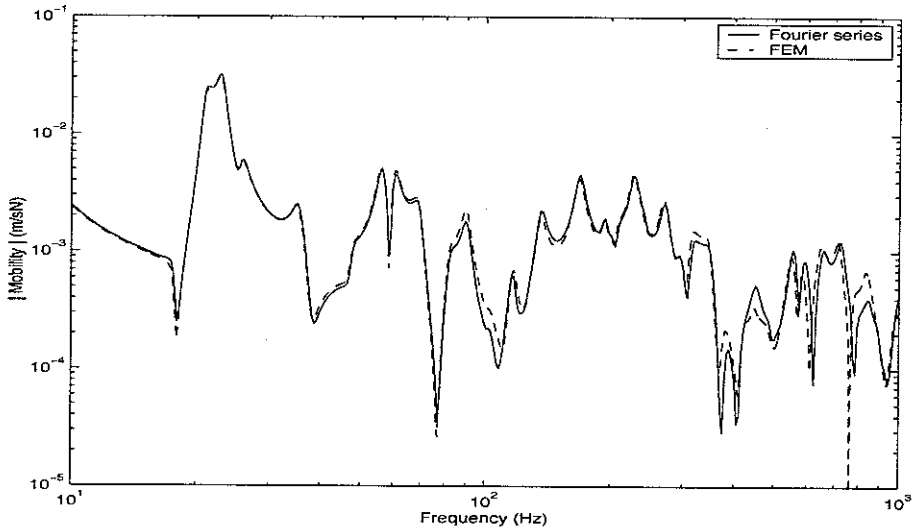

Figure 23. Transfer mobility for the plate (at x = 1.51 m and y = 0.50 m) in the built-up finite beam/plate structure as in Figure 20 ($\eta_p = 0.05$ in the plate, $\eta_b = 0.05$ in the beam, point force applied at $x = 0$).

4.3.2 Power balance

The total input power and the net power transferred to the plate are compared in Figure 24 for the structure shown in Figure 20. It is clear that the total power input is greater than the power transferred from the beam to the plate at all frequencies.

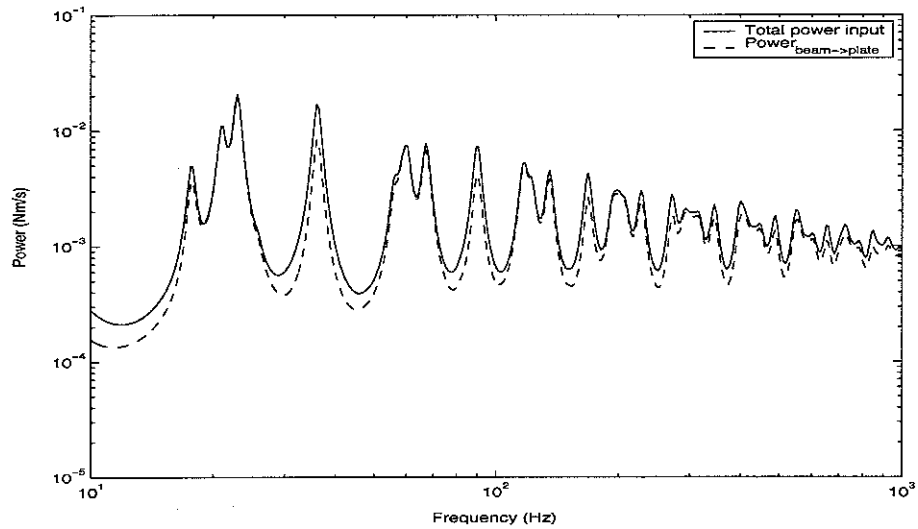

Figure 24. Comparison of total input power inserted to the coupled structure shown in Figure 20 and net power transferred to the plate ($\eta_p = 0.05$ in the plate, $\eta_b = 0.05$ in the beam, point force applied at $x = 0$).

From Figure 21, if the dissipated power in the beam is added to the transferred power, it is expected that the result should be equal to the total input power. Figure 25 shows that excellent agreement is found for this overall power balance. The maximum error between the two curves is 0.4 %, which occurs due to errors from the numerical integration.

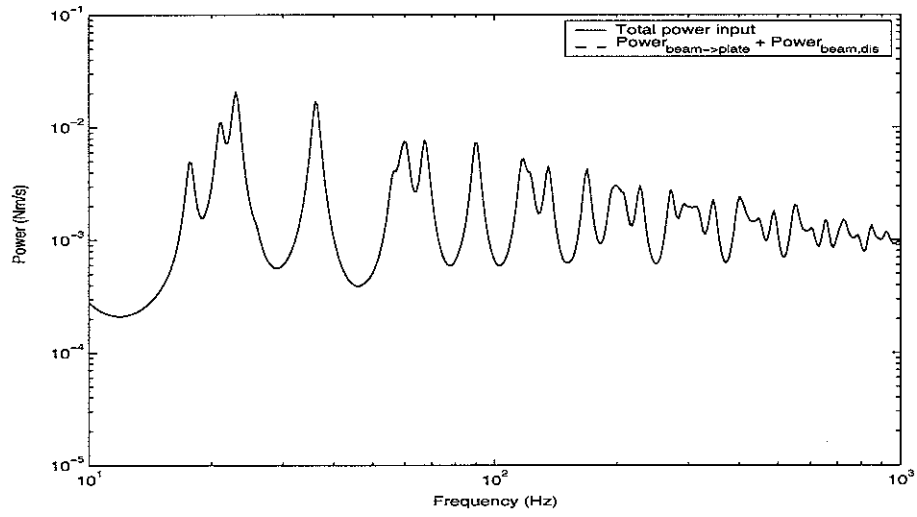

Figure 25. Comparison of power balance for the beam of the built-up structure shown in Figure 20 ($\eta_p = 0.05$ in the plate, $\eta_b = 0.05$ in the beam, point force applied at $x = 0$ of beam).

In addition to the power balance for the beam, the power relationship for the plate is also investigated and is presented in Figure 26.

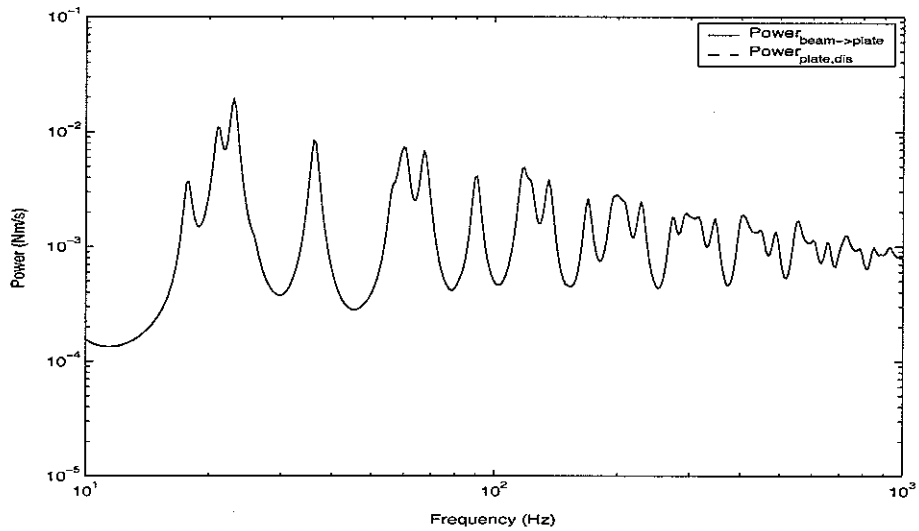

Figure 26. Comparison of power balance for the plate of the built-up structure shown in Figure 20 ($\eta_p = 0.05$ in the plate, $\eta_b = 0.05$ in the beam, point force applied at $x = 0$ of beam).

Again this shows good agreement between the net transferred power and the power dissipated in the plate. The maximum error between the two curves is 1.4 %. This indicates that the strain energy of the plate is appropriate for obtaining the power dissipated in plate as assumed before. Note that in the wave method, the energy conservation for the plate seemed to be violated when the travelling and the nearfield wave were both considered [1]. Thus, it can be said that the Fourier series method is a good alternative to identify the energy relationship between subsystems in the coupled structure and to predict accurately the coupled response.

5. INFINITE BEAM COUPLED TO FINITE WIDTH PLATE: PLATE-EXCITED

5.1 Coupling between infinitely long structure

In the previous sections 2, 3 and 4, the built-up structures considered had excitation applied to the beam. Similarly, a plate-excited case for the same structures can be analysed. In this section, firstly an infinite beam and infinitely long finite width plate are considered. The plate is divided into two components $p1$ and $p2$ so that the external force can be defined based on force equilibrium conditions. For the finite width plate a pinned boundary condition is considered as before, and the coupled structure and the corresponding force relationships are illustrated in Figure 27.

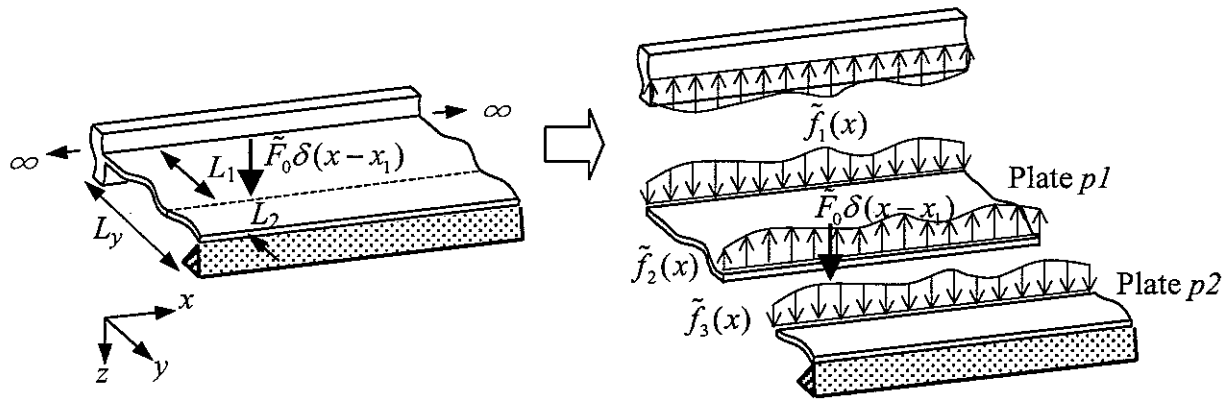

Figure 27. A built-up structure consisting of an infinite beam attached to a finite width plate where the plate is excited.

As before, a force per unit length $\tilde{f}_1(x)$ acts between the plate and the beam as in Figure 27. The point force is acting on the plate located at $x=x_1$, $y=L_1$ and therefore the point force is defined by $\tilde{F}_0\delta(x-x_1)\delta(y-L_1)$ where δ is the Dirac delta function.

The analysis for the coupled structure can start from the equation of motion of the beam with damping as follows.

$$\tilde{D}_b \frac{\partial^4 \tilde{w}_b(x)}{\partial x^4} - m_b'\omega^2 \tilde{w}_b(x) = -\tilde{f}_1(x) \tag{5.1}$$

where $\tilde{D}_b$ is bending stiffness and m_b' is its mass per unit length and the corresponding Fourier transform of equation (5.1) is

$$\tilde{D}_b k_x^4 \tilde{W}_b(k_x) - m_b'\omega^2 \tilde{W}_b(k_x) = -\tilde{F}_1(k_x). \tag{5.2}$$

where $\tilde{F}_1(k_x)$ is the Fourier transform of $\tilde{f}_1(x)$.

Also, the equation of motion of the free plate with damping is

$$\tilde{D}_p\left(\frac{\partial^4\tilde{w}_p(x,y)}{\partial x^4}+2\frac{\partial^4\tilde{w}_p(x,y)}{\partial x^2\partial y^2}+\frac{\partial^4\tilde{w}_p(x,y)}{\partial y^4}\right)-m_p''\omega^2\tilde{w}_p(x,y)=0, \tag{5.3}$$

and the corresponding Fourier transform of equation (5.3) is

$$\tilde{D}_p\left\{k_x^4\tilde{W}_p(k_x,y)-2k_x^2\frac{\partial^2\tilde{W}_p(k_x,y)}{\partial y^2}+\frac{\partial^4\tilde{W}_p(k_x,y)}{\partial y^4}\right\}-m_p'\omega^2\tilde{W}_p(k_x,y)=0. \tag{5.4}$$

If harmonic waves in the plates are assumed, the wavenumber relationship can be defined as before. The wave propagating or decaying away from the junction can be defined as

$$k_y=-\sqrt{k_x^2-\tilde{k}_p^2}=\tilde{k}_{y1}, \tag{5.5a}$$

$$k_y=-\sqrt{k_x^2+\tilde{k}_p^2}=\tilde{k}_{y2}. \tag{5.5b}$$

Meanwhile, the positive square roots are assumed for waves travelling towards the junction of beam 1 and the plate and are found to be

$$k_y=\sqrt{k_x^2-\tilde{k}_p^2}=\tilde{k}_{y3}, \tag{5.5c}$$

$$k_y=\sqrt{k_x^2+\tilde{k}_p^2}=\tilde{k}_{y4}. \tag{5.5d}$$

If $|k_x|<|\tilde{k}_p|$, then wavenumbers $\tilde{k}_{y1}$ and $\tilde{k}_{y3}$ are considered as travelling waves, and $\tilde{k}_{y2}$ and $\tilde{k}_{y4}$ are considered as nearfield waves. Conversely, if $|k_x|>|\tilde{k}_p|$, then all of them behave as nearfield waves.

Then the motion of the plate $p1$ can be written as

$$\tilde{W}_{p1}(k_x,y_1)=\tilde{B}_1e^{\tilde{k}_{y1}y_1}+\tilde{B}_2e^{\tilde{k}_{y2}y_1}+\tilde{B}_3e^{\tilde{k}_{y3}y_1}+\tilde{B}_4e^{\tilde{k}_{y4}y_1} \tag{5.6}$$

and for the plate $p2$,

$$\tilde{W}_{p2}(k_x, y_2) = \tilde{C}_1 e^{\tilde{k}_{y1} y_2} + \tilde{C}_2 e^{\tilde{k}_{y2} y_2} + \tilde{C}_3 e^{\tilde{k}_{y3} y_2} + \tilde{C}_4 e^{\tilde{k}_{y4} y_2} \tag{5.7}$$

Note that different local coordinate systems are used in equations (5.6) and (5.7) in describing the motion of the plate i.e. $y_1 (\equiv y)$ for plate $p1$ and $y_2 (\equiv y - L_1)$ for plate $p2$.

The response of the beam and the plates can be obtained based on appropriate boundary conditions.

(i) Continuity equation for the beam and plate $p1$; equal displacement to the plate at $y_1 = 0$ of plate $p1$

$$\tilde{W}_{p1}(k_x, y)\Big|_{y=0} = \tilde{W}_b(k_x) \tag{5.8}$$

$$\tilde{B}_1 + \tilde{B}_2 + \tilde{B}_3 + \tilde{B}_4 - \tilde{W}_{b1}(k_x) = 0. \tag{5.9}$$

(ii) Sliding condition; the beam is assumed infinitely stiff to torsion along $y_1 = 0$ of plate $p1$

$$\frac{\partial \tilde{W}_{p1}(k_x, y_1)}{\partial y_1}\bigg|_{y=0} = 0 \tag{5.10}$$

$$\frac{\partial \tilde{W}_{p1}(k_x, y_1)}{\partial y_1}\bigg|_{y=0} = \tilde{B}_1 \tilde{k}_{y1} + \tilde{B}_2 \tilde{k}_{y2} + \tilde{B}_3 \tilde{k}_{y3} + \tilde{B}_4 \tilde{k}_{y4} = 0. \tag{5.11}$$

(iii) Force equilibrium condition; the force on the plate are equal and opposite to the respective force on the beam

$$\tilde{D}_p \left[\frac{\partial^3 \tilde{W}_{p1}(k_x, y_1)}{\partial y_1^3} - k_x^2 (2 - \nu) \frac{\partial \tilde{W}_{p1}(k_x, y_1)}{\partial y_1} \right]_{y_1=0} = \tilde{F}_1(k_x) \tag{5.12}$$

Combining equation (5.2) and (5.12) results in

$$-\tilde{D}_p \left[\frac{\partial^3 \tilde{W}_{p1}(k_x, y_1)}{\partial y_1^3} - k_x^2 (2 - \nu) \frac{\partial \tilde{W}_{p1}(k_x, y_1)}{\partial y_1} \right]_{y_1=0} = \left(\tilde{D}_b k_x^4 - m_b' \omega^2 \right) \tilde{W}_b(k_x). \tag{5.13}$$

Substituting equation (5.10) into equation (5.13), simpler form is obtained as

$$-\tilde{D}_p \left[\frac{\partial^3 \tilde{W}_{p1}(k_x, y_1)}{\partial y_1^3} \right]_{y_1=0} = \left(\tilde{D}_b k_x^4 - m_b' \omega^2 \right) \tilde{W}_b(k_x). \tag{5.14}$$

Therefore,

$$\tilde{D}_p\left(\tilde{k}_{y1}^3\tilde{B}_1+\tilde{k}_{y2}^3\tilde{B}_2+\tilde{k}_{y3}^3\tilde{B}_3+\tilde{k}_{y4}^3\tilde{B}_4\right)+\left(\tilde{D}_b k_x^4-m_b'\omega^2\right)\tilde{W}_b(k_x)=0. \tag{5.15}$$

(iv) Continuity equation for plate $p1$ and plate $p2$; equal displacement at junction $y_1=L_1$ of plate $p1$ and $y_2=0$ of plate $p2$

$$\tilde{W}_{p1}(k_x,y)\Big|_{y_1=L_1}=\tilde{W}_{p2}(k_x,y)\Big|_{y_2=0} \tag{5.16}$$

$$\tilde{B}_1e^{\tilde{k}_{y1}L_1}+\tilde{B}_2e^{\tilde{k}_{y2}L_1}+\tilde{B}_3e^{\tilde{k}_{y3}L_1}+\tilde{B}_4e^{\tilde{k}_{y4}L_1}-\tilde{C}_1-\tilde{C}_2-\tilde{C}_3-\tilde{C}_4=0 \tag{5.17}$$

(v) Continuity equation for plate $p1$ and plate $p2$; equal rotational displacement at junction $y_1=L_1$ of plate $p1$ and $y_2=0$ of plate $p2$

$$\frac{\partial\tilde{W}_{p1}(k_x,y_1)}{\partial y_1}\Bigg|_{y_1=L_1}=\frac{\partial\tilde{W}_{p2}(k_x,y_2)}{\partial y_2}\Bigg|_{y_2=0} \tag{5.18}$$

$$\tilde{B}_1\tilde{k}_{y1}e^{\tilde{k}_{y1}L_1}+\tilde{B}_2\tilde{k}_{y2}e^{\tilde{k}_{y2}L_1}+\tilde{B}_3\tilde{k}_{y3}e^{\tilde{k}_{y3}L_1}+\tilde{B}_4\tilde{k}_{y4}e^{\tilde{k}_{y4}L_1}-\tilde{C}_1\tilde{k}_{y1}-\tilde{C}_2\tilde{k}_{y2}-\tilde{C}_3\tilde{k}_{y3}-\tilde{C}_4\tilde{k}_{y4}=0 \tag{5.19}$$

(vi) Moment equilibrium condition; the moments acting on plates $p1$ and $p2$ are equal at junction $y=L_1$

$$\tilde{M}_{p1}(k_x,y_1)\Big|_{y_1=L_1}=\tilde{M}_{p2}(k_x,y_2)\Big|_{y_2=0} \tag{5.20}$$

where $\tilde{M}_p(k_x,y_i)$ is the Fourier transform of the moment per unit length $\tilde{m}_p(x,y_i)$ acting on edges of a plate and given by

$$\tilde{M}_p(k_x,y_i)=\tilde{D}_p\left[\frac{\partial^2\tilde{W}_p(k_x,y_i)}{\partial y_i^2}-k_x^2\nu\tilde{W}_p(k_x,y_i)\right],\ i=1,2. \tag{5.21}$$

Therefore,

$$\begin{aligned}&\tilde{D}_p\left[\tilde{B}_1\left(\tilde{k}_{y1}^2-k_x^2\nu\right)e^{\tilde{k}_{y1}L_1}+\tilde{B}_2\left(\tilde{k}_{y2}^2-k_x^2\nu\right)e^{\tilde{k}_{y2}L_1}+\tilde{B}_3\left(\tilde{k}_{y3}^2-k_x^2\nu\right)e^{\tilde{k}_{y3}L_1}+\tilde{B}_4\left(\tilde{k}_{y4}^2-k_x^2\nu\right)e^{\tilde{k}_{y4}L_1}\right]\\&-\tilde{D}_p\left[\tilde{C}_1\left(\tilde{k}_{y1}^2-k_x^2\nu\right)+\tilde{C}_2\left(\tilde{k}_{y2}^2-k_x^2\nu\right)+\tilde{C}_3\left(\tilde{k}_{y3}^2-k_x^2\nu\right)+\tilde{C}_4\left(\tilde{k}_{y4}^2-k_x^2\nu\right)\right]=0.\end{aligned} \tag{5.22}$$

(vii) Force equilibrium condition; the forces acting at junction $y_1 = L_1$ of plate $p1$ and $y = 0$ of plate $p2$ should be in equilibrium with the applied external force as shown in Figure 27

$$-\tilde{F}_2(k_x, y_1)\Big|_{y=L_1} + \tilde{F}_3(k_x, y_2)\Big|_{y=0} = \tilde{F}_0(k_x) \tag{5.23}$$

where $\tilde{F}_2(k_x, y_1)$, $\tilde{F}_3(k_x, y_2)$ and $\tilde{F}_0(k_x)$ are the Fourier transforms of the forces $\tilde{f}_2(x, y_1)$, $\tilde{f}_3(x, y_2)$ and $\tilde{F}_0(x - x_1)$ respectively.

Therefore,

$$\begin{aligned} &-\tilde{D}_p\left[\frac{\partial^3 \tilde{W}_{p1}(k_x, y_1)}{\partial y_1^3} - k_x^2(2-\nu)\frac{\partial \tilde{W}_{p1}(k_x, y_1)}{\partial y_1}\right]_{y_1=L_1} \\ &+\tilde{D}_p\left[\frac{\partial^3 \tilde{W}_{p2}(k_x, y_2)}{\partial y_2^3} - k_x^2(2-\nu)\frac{\partial \tilde{W}_{p2}(k_x, y_2)}{\partial y_2}\right]_{y_2=0} = \tilde{F}_0(k_x). \end{aligned} \tag{5.24}$$

$$\begin{aligned} &-\tilde{D}_p\begin{bmatrix} \tilde{B}_1\left\{\tilde{k}_{y1}^3 - k_x^2(2-\nu)\tilde{k}_{y1}\right\}e^{\tilde{k}_{y1}L_1} + \tilde{B}_2\left\{\tilde{k}_{y2}^3 - k_x^2(2-\nu)\tilde{k}_{y2}\right\}e^{\tilde{k}_{y2}L_1} \\ +\tilde{B}_3\left\{\tilde{k}_{y3}^3 - k_x^2(2-\nu)\tilde{k}_{y3}\right\}e^{\tilde{k}_{y3}L_1} + \tilde{B}_4\left\{\tilde{k}_{y4}^3 - k_x^2(2-\nu)\tilde{k}_{y4}\right\}e^{\tilde{k}_{y4}L_1} \end{bmatrix} \\ &+\tilde{D}_p\begin{bmatrix} \tilde{C}_1\left\{\tilde{k}_{y1}^3 - k_x^2(2-\nu)\tilde{k}_{y1}\right\} + \tilde{C}_2\left\{\tilde{k}_{y2}^3 - k_x^2(2-\nu)\tilde{k}_{y2}\right\} \\ +\tilde{C}_3\left\{\tilde{k}_{y3}^3 - k_x^2(2-\nu)\tilde{k}_{y3}\right\} + \tilde{C}_4\left\{\tilde{k}_{y4}^3 - k_x^2(2-\nu)\tilde{k}_{y4}\right\} \end{bmatrix} = \tilde{F}_0(k_x). \end{aligned} \tag{5.25}$$

(viii) Pinned condition; no moment is acting on the edge of $y_2 = L_2$ of plate $p2$

$$\tilde{M}_{p2}(k_x, y)\Big|_{y_2=L_2} = 0 \tag{5.26}$$

$$\tilde{D}_p\left[\tilde{C}_1\left(\tilde{k}_{y1}^2 - k_x^2\nu\right)e^{\tilde{k}_{y1}L_2} + \tilde{C}_2\left(\tilde{k}_{y2}^2 - k_x^2\nu\right)e^{\tilde{k}_{y2}L_2} + \tilde{C}_3\left(\tilde{k}_{y3}^2 - k_x^2\nu\right)e^{\tilde{k}_{y3}L_2} + \tilde{C}_4\left(\tilde{k}_{y4}^2 - k_x^2\nu\right)e^{\tilde{k}_{y4}L_2}\right] = 0. \tag{5.27}$$

(ix) Pinned condition; the displacement along $y_2 = L_2$ of plate $p2$ is zero

$$\tilde{W}_{p2}(k_x, y_2)\Big|_{y_2=L_2} = 0. \tag{5.28}$$

$$\tilde{C}_1 e^{\tilde{k}_{y1}L_2} + \tilde{C}_2 e^{\tilde{k}_{y2}L_2} + \tilde{C}_3 e^{\tilde{k}_{y3}L_2} + \tilde{C}_4 e^{\tilde{k}_{y4}L_2} = 0 \tag{5.29}$$

Equations representing boundary conditions (5.9), (5.11), (5.15), (5.17), (5.19), (5.22), (5.25), (5.27) and (5.29) can be incorporated into a matrix form. For simplification, new variables α_i and β_i are introduced as follows.

$$\begin{aligned}
\alpha_1 &= \tilde{k}_{y1}^3 - k_x^2(2-\nu)\tilde{k}_{y1}, \\
\alpha_2 &= \tilde{k}_{y2}^3 - k_x^2(2-\nu)\tilde{k}_{y2}, \\
\alpha_3 &= \tilde{k}_{y3}^3 - k_x^2(2-\nu)\tilde{k}_{y3}, \\
\alpha_4 &= \tilde{k}_{y4}^3 - k_x^2(2-\nu)\tilde{k}_{y4}.
\end{aligned} \tag{5.30}$$

$$\begin{aligned}
\beta_1 &= \tilde{k}_{y1}^2 - k_x^2\nu, \\
\beta_2 &= \tilde{k}_{y2}^2 - k_x^2\nu, \\
\beta_3 &= \tilde{k}_{y3}^2 - k_x^2\nu, \\
\beta_4 &= \tilde{k}_{y4}^2 - k_x^2\nu.
\end{aligned} \tag{5.31}$$

Then, the matrix form of the equations relating the boundary conditions in the wavenumber domain is

$$\mathbf{Ku} = \mathbf{F} \tag{5.32}$$

where the dynamic stiffness matrix $\mathbf{K}$ is

$$\mathbf{K}=\begin{bmatrix}
1 & 1 & 1 & 1 & 0 & 0 & 0 & 0 & -1 \\
\tilde{k}_{y1} & \tilde{k}_{y2} & \tilde{k}_{y3} & \tilde{k}_{y4} & 0 & 0 & 0 & 0 & 0 \\
\tilde{D}_p\tilde{k}_{y1}^3 & \tilde{D}_p\tilde{k}_{y2}^3 & \tilde{D}_p\tilde{k}_{y3}^3 & \tilde{D}_p\tilde{k}_{y4}^3 & 0 & 0 & 0 & 0 & \tilde{K}_b \\
e^{\tilde{k}_{y1}L_1} & e^{\tilde{k}_{y2}L_1} & e^{\tilde{k}_{y3}L_1} & e^{\tilde{k}_{y4}L_1} & -1 & -1 & -1 & -1 & 0 \\
\tilde{k}_{y1}e^{\tilde{k}_{y1}L_1} & \tilde{k}_{y2}e^{\tilde{k}_{y2}L_1} & \tilde{k}_{y3}e^{\tilde{k}_{y3}L_1} & \tilde{k}_{y4}e^{\tilde{k}_{y4}L_1} & -\tilde{k}_{y1} & -\tilde{k}_{y2} & -\tilde{k}_{y3} & -\tilde{k}_{y4} & 0 \\
\beta_1 e^{\tilde{k}_{y1}L_1} & \beta_2 e^{\tilde{k}_{y2}L_1} & \beta_3 e^{\tilde{k}_{y3}L_1} & \beta_4 e^{\tilde{k}_{y4}L_1} & -\beta_1 & -\beta_2 & -\beta_3 & -\beta_4 & 0 \\
-\alpha_1 e^{\tilde{k}_{y1}L_1} & -\alpha_2 e^{\tilde{k}_{y2}L_1} & -\alpha_3 e^{\tilde{k}_{y3}L_1} & -\alpha_4 e^{\tilde{k}_{y4}L_1} & \alpha_1 & \alpha_2 & \alpha_3 & \alpha_4 & 0 \\
0 & 0 & 0 & 0 & \beta_1 e^{\tilde{k}_{y1}L_2} & \beta_2 e^{\tilde{k}_{y2}L_2} & \beta_3 e^{\tilde{k}_{y3}L_2} & \beta_4 e^{\tilde{k}_{y4}L_2} & 0 \\
0 & 0 & 0 & 0 & e^{\tilde{k}_{y1}L_2} & e^{\tilde{k}_{y2}L_2} & e^{\tilde{k}_{y3}L_2} & e^{\tilde{k}_{y4}L_2} & 0
\end{bmatrix}, \tag{5.33}$$

where $\tilde{K}_b = \tilde{D}_b k_x^4 - m_b'\omega^2$. Also, the displacement vector $\mathbf{u}$ is

$$\mathbf{u} = \left[\tilde{B}_1(k_x) \quad \tilde{B}_2(k_x) \quad \tilde{B}_3(k_x) \quad \tilde{B}_4(k_x) \quad \tilde{C}_1(k_x) \quad \tilde{C}_2(k_x) \quad \tilde{C}_3(k_x) \quad \tilde{C}_4(k_x) \quad \tilde{W}_b(k_x) \right]^T, \tag{5.34}$$

and the force vector is

$$\mathbf{F} = \left[0 \quad 0 \quad 0 \quad 0 \quad 0 \quad 0 \quad \tilde{F}_0(k_x) \quad 0 \quad 0 \right]^T. \tag{5.35}$$

Therefore, the response of the beam and the plates can be obtained from solution of equation (5.32), as follows, if the excitation force is known.

$$\mathbf{u} = \mathbf{K}^{-1}\mathbf{F} \tag{5.36}$$

5.2 Numerical analysis

Before mentioning a finite beam coupled structure, the numerical analysis of the infinite beam coupled to the finite width plate is carried out in this section. The structure is exactly identical with the structure explained in section 3.2 except that the external force is applied on the plate. Here, the excitation is applied at $x = 0$ and $y = 0.5$. The other boundary conditions are also the same as before.

The same FEM model presented in section 3.2 is used to compare the dynamic response. While the external force is applied at $x = 0$ and $y = 0.5$ of the one sliding plate edge, the other opposite edge ($x = 8.0\,\mathrm{m}$) is assumed to be free with gradually changing structural damping ($\eta_p = 0.05 \sim 0.65$) as well. Also, for comparison, half the external force is used in FEM as the analytical model is the infinite beam coupled structure. In Figure 28, the point mobilities are compared. It can be seen that they agree well except at low frequencies. As explained before in section 3.2, this is again due to the global modes of the finite model of the FEM.

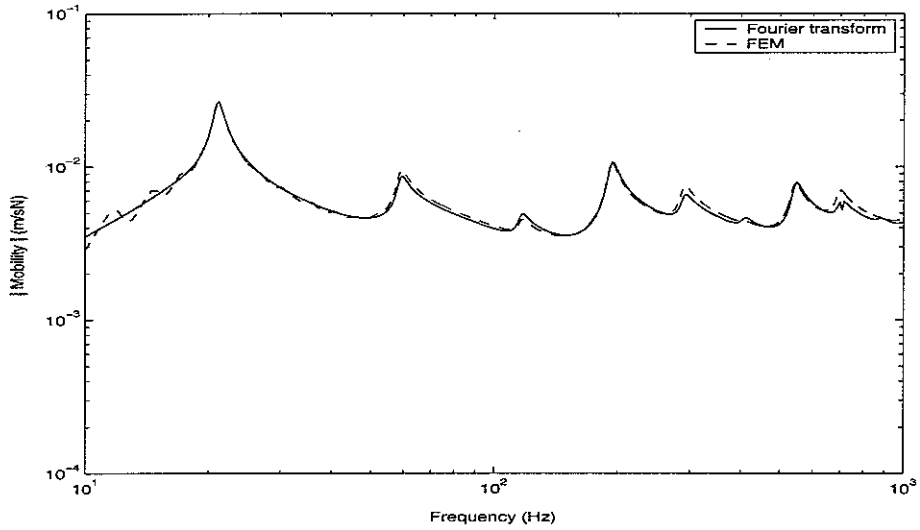

Figure 28. Comparison of the point mobility calculated by Fourier transform and FEM for the infinite beam and finite plate as in Figure 27 (point force applied at $x = 0$ and $y = 0.5$). Non-dimensional wavenumber $\gamma = -50$ to 50 are used in the inverse Fourier transform.

6. FINITE BEAM COUPLED TO FINITE PLATE: PLATE –EXCITED

6.1 Response and power balance

Just as the response of the infinite coupled structure was investigated based on the Fourier transform technique in the previous section, the response of the finite structure can be obtained based on the Fourier series, as explained in earlier section 4.1. The coupled structure consisting of finite subsystems is shown in Figure 29 where the ends of the finite beam and two edges of the plate at $x=0$ and $x=L_x$ are considered to be sliding. The other boundary conditions of the junction and the opposite edge parallel to the beam are the same as before.

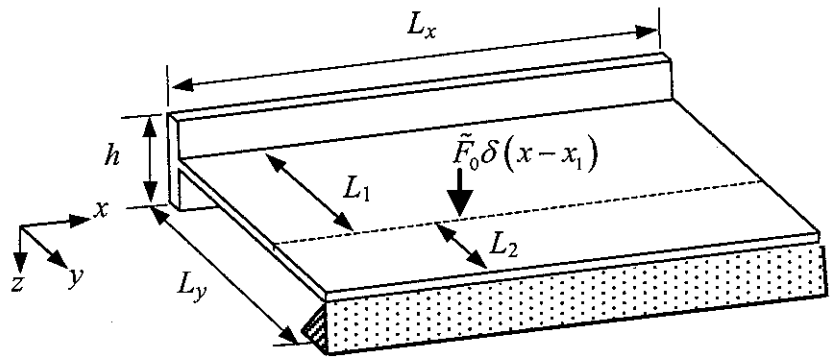

Figure 29. A built-up structure consisting of a finite beam and a rectangular plate excited by a point force.

The behaviour of the coupled finite beam and the rectangular plate can be described in terms of cosine orders as explained in section 4.1. Therefore, the responses of the finite beam and the plate are given by equations (4.4) and (4.5) respectively.

It is important to note that the external point force should be described in terms of its spatial Fourier series as follows.

$$\tilde{F}_0\delta(x-x_1)=\frac{\tilde{F}_0(k_{x,0})}{2}+\sum_{n=1}^{\infty}\tilde{F}_0(k_{x,n})\cos(k_{x,n}x) \tag{6.1}$$

where $\tilde{F}_0(k_{x,n})$ is the Fourier transformed point force and is defined by

$$\tilde{F}_0(k_x)=\frac{2}{L_x}\sum_{n=0}^{\infty}\tilde{F}_0\cos(k_{x,n}x_1)=\tilde{F}_0\frac{2}{L_x}\sum_{n=0}^{\infty}\cos(k_{x,n}x_1) \tag{6.2}$$

where $\tilde{F}_0$ is the point force, x_1 is the coordinate where the point force is applied, L_x is the length of the beam and $k_{x,n} = n\pi/L_x$ is the n^{th} trace wavenumber along the beam.

The power balance should also be maintained for the coupled structure. The power flow similar to Figure 21 can be presented and shown in Figure 30.

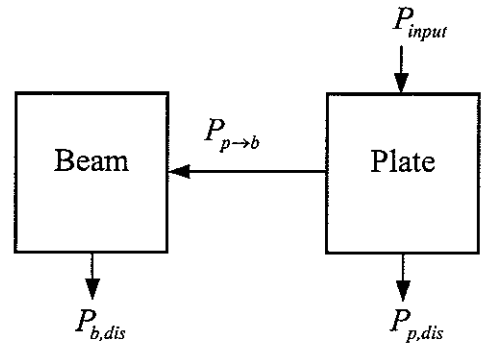

Figure 30. Power balance between subsystems of the coupled structure as shown in Figure 29.

In the figure, $P_{b,dis}$ and $P_{p,dis}$ are the power dissipated in the beam and the plate respectively and are obtained from strain energies of the subsystem as well. Note that $P_{p\to b}$ is net power transferred from the excited plate to the beam and is given by

$$P_{p\to b} = \frac{1}{2}\int_0^{L_x} \mathrm{Re}\left\{\tilde{f}_1(x)^* \times i\omega\tilde{w}_b(x)\right\}dx . \qquad (6.3)$$

Most of the equations related to the power balance are the same as presented in section 4.2. However, the response of the plate is given by equations (5.6) and (5.7) in the local coordinates for its two parts. Therefore, equations related to the stain energy of a subsystem such as (4.14) are expressed in the local coordinate system of each plate part.

6.2 Numerical analysis

6.2.1 Response of the coupled structure

Numerical analysis has been carried out for the coupled structure shown in Figure 29 where an external force is applied to the plate. The dimensions of the coupled structure are not changed, and are presented in Table 2.

As before, the external point force considered has unit magnitude ($\tilde{F}_0 = 1$). To enable comparison, the force is applied at $x = 1.51$ m, $y = 0.50$ m on the plate, which corresponds to

the response point shown when the force was applied to the beam in section 4. 400 components ($n = 400$) of the Fourier series are considered in calculation as before.

Firstly, the point mobility is compared with the result of FEM in Figure 31. The results are in good agreement.

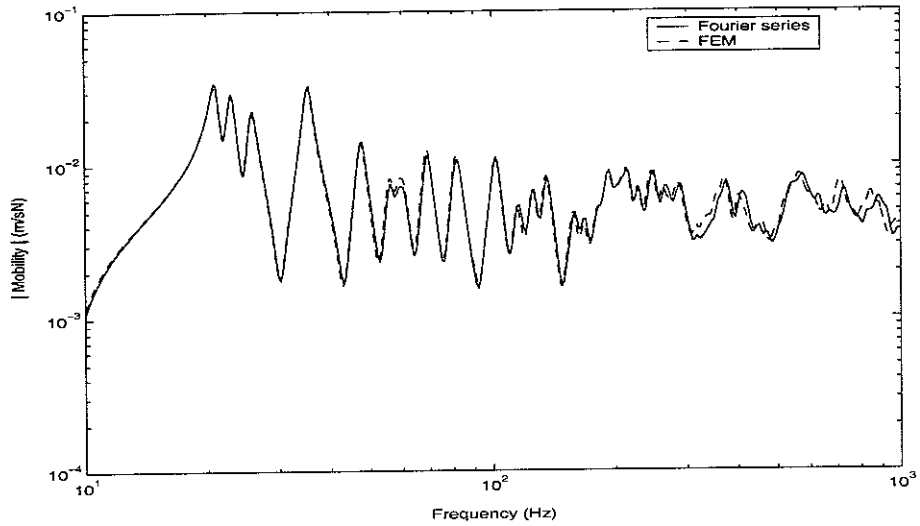

Figure 31. Point mobility comparison for the plate-excited coupled structure as in Figure 29 ($\eta_p = 0.05$ in the plate, $\eta_b = 0.05$ in the beam, point force applied at $x = 1.51$ m, $y = 0.50$ m on the plate).

Next, the transfer mobility is presented in Figure 32 for the response at $x = 0.0$ m on the beam. This is shown with the result from FEM and shows good agreement as well.

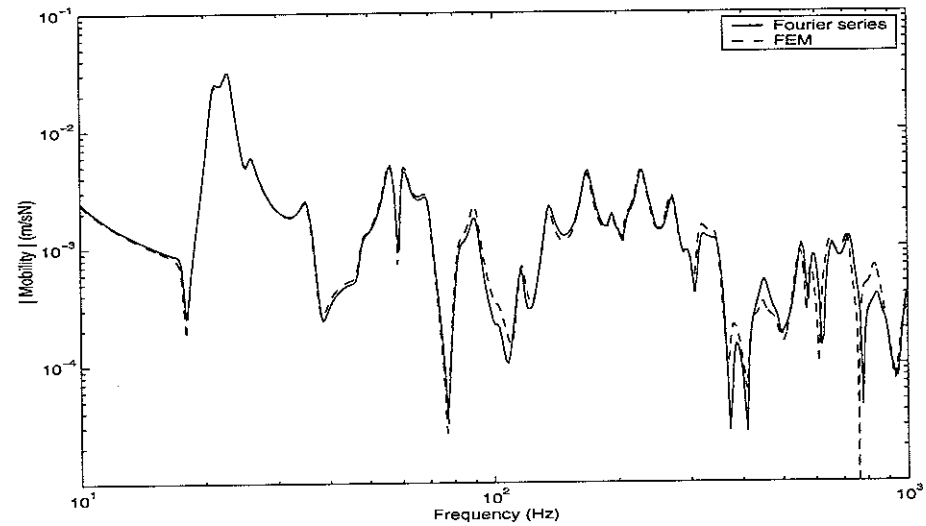

Figure 32. Transfer mobility comparison for the plate-excited coupled structure as in Figure 29 ($\eta_p = 0.05$ in the plate, $\eta_b = 0.05$ in the beam, response at $x = 0.0$ m of the beam, point force applied at $x = 1.51$ m, $y = 0.50$ m).

In addition, in Figure 33, this plate-excited result based on the Fourier series from Figure 32 is compared with the beam-excited result presented in section 4.3.1 (see Figure 23). They are in good agreement, which one would expect from the principle of reciprocity [13] i.e. $\dot{w}_b(x=0)/f_p(x_p,y_p) = \dot{w}_p(x_p,y_p)/f_b(x=0)$.

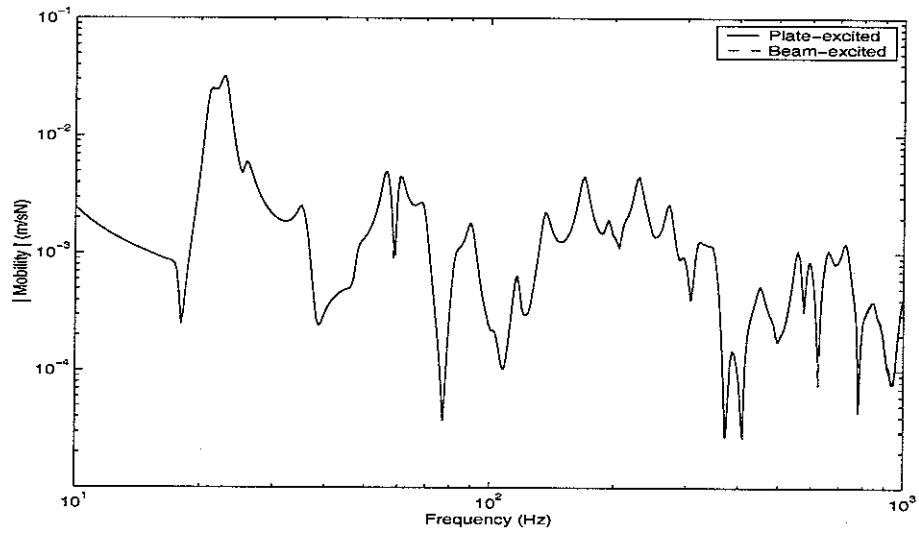

Figure 33. Transfer mobility comparison between the plate-excited structure as in Figure 29 and the beam-excited structure as in Figure 20 ($\eta_p = 0.05$ in the plate, $\eta_b = 0.05$ in the beam, transfer mobility between $x = 0.0$ m of the beam and $x = 1.51$ m, $y = 0.50$ m on the plate).

6.2.2 Power balance

To examine the power balance relationship, the relevant powers represented in Figure 30 have been calculated and compared in this section. Firstly, the total input power and the power transferred from the plate to the beam are compared in Figure 34. Comparing this with Figure 24 where the beam is excited, it can be seen that the difference between the two powers in Figure 34 is much larger than that in Figure 24 as most power is dissipated in the plate and not transferred to the beam.

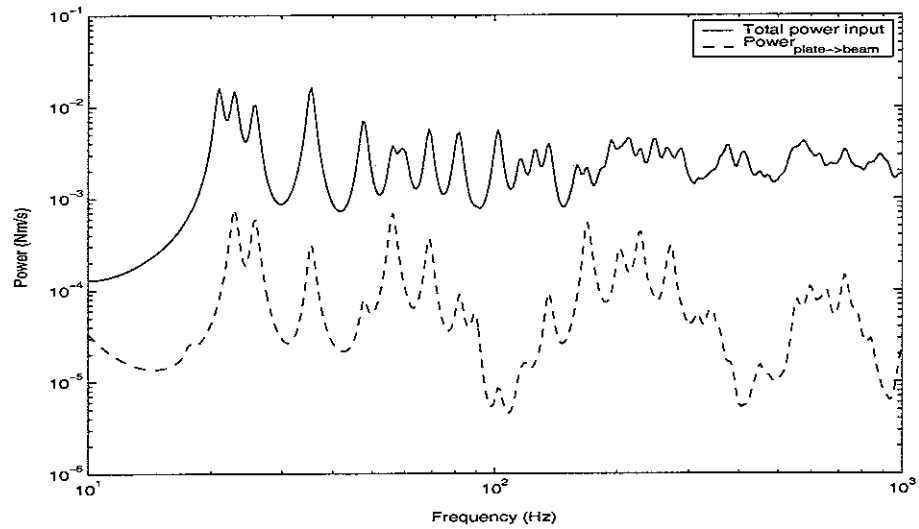

Figure 34. Comparison of total input power to the coupled structure shown in Figure 29 and net power transferred to the beam ($\eta_p = 0.05$ in the plate, $\eta_b = 0.05$ in the beam, point force applied at $x = 1.51$ m, $y = 0.50$ m on the plate).

In Figure 35, the sum of the dissipated power in the plate and the transferred power is compared with the total input power. They show good agreement with a maximum error of 0.5 %, which shown that the power balance for the plate holds, verifying the model used.

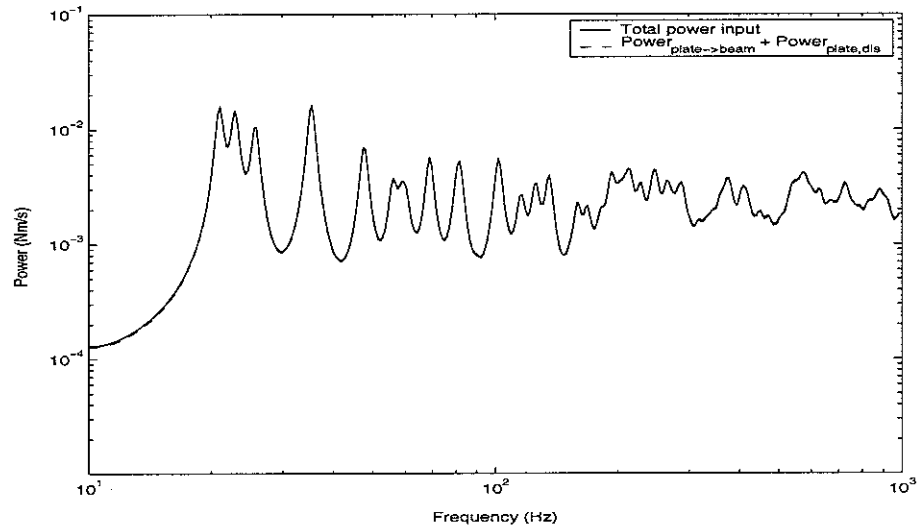

Figure 35. Comparison of power balance for the plate of the built-up structure shown in Figure 29 ($\eta_p = 0.05$ in the plate, $\eta_b = 0.05$ in the beam, point force applied at $x = 1.51$ m, $y = 0.50$ m on the plate).

Finally, the power balance for the beam is investigated by comparing the net transferred power and the dissipated power in the beam in Figure 36. It can be seen that two curves are identical (maximum error is 0.0 %) and the power balance for the beam is maintained.

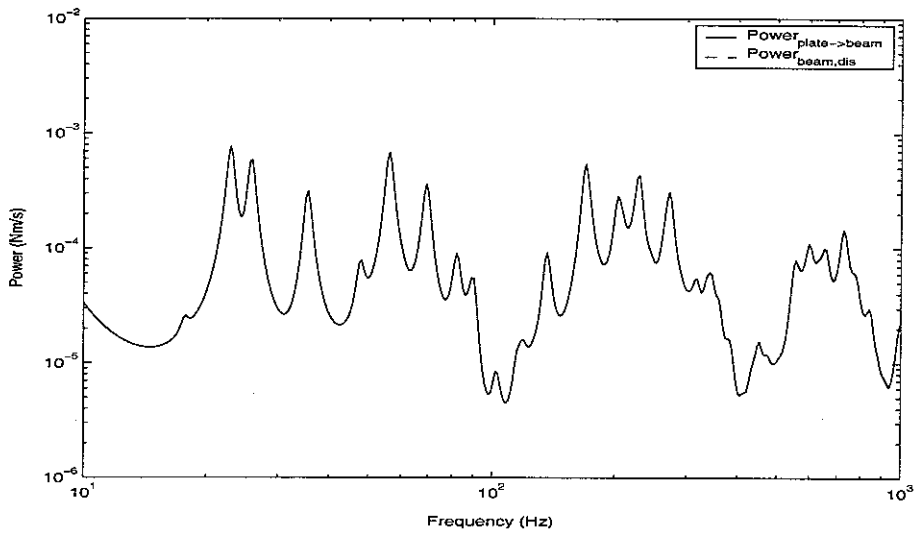

Figure 36. Comparison of power balance for the beam of the built-up structure shown in Figure 29 ($\eta_p = 0.05$ in the plate, $\eta_b = 0.05$ in the beam, point force applied at $x = 1.51$ m, $y = 0.50$ m on the plate).

7. TWO PARALLEL BEAMS COUPLED BY A FINITE WIDTH PLATE

7.1 Coupling between infinitely long structures

The behaviour of a symmetric two-beam structure was analysed previously using the wave method [1]. In this method, the response was obtained by the synthesis of anti-symmetric and symmetric responses of the single beam-plate structure, which is not applicable to the case when the two-beam structure is not exactly symmetric. Using the Fourier technique, this difficulty can be readily overcome. The two-beam structure consisting of two infinite beams and an infinitely long finite width plate and their force relationships are shown in Figure 37. As before, harmonic motion at frequency ω is assumed. It is again assumed for simplicity that the beams are infinitely stiff to torsion along $y = 0$ and $y = L_y$.

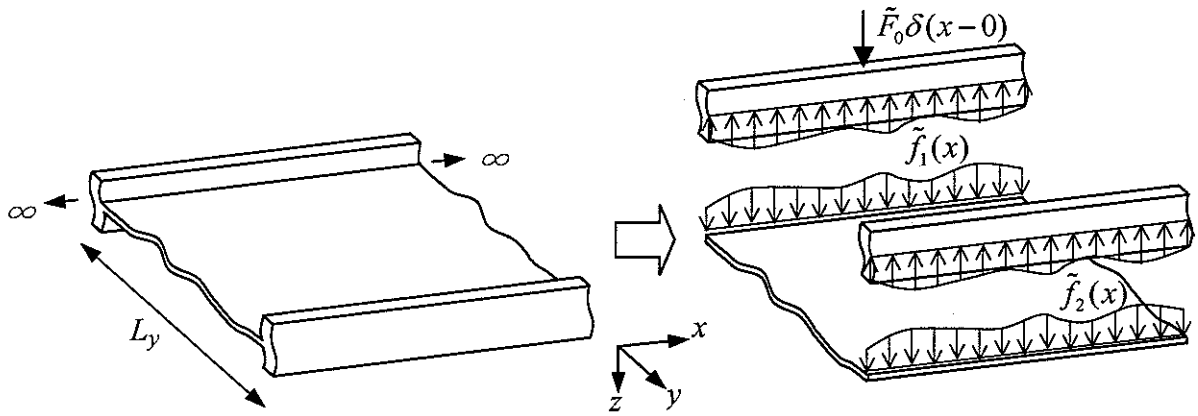

Figure 37. A built-up structure consisting of infinite two beams attached to an infinitely long finite width plate and force relationship between them.

When the infinitely long finite width plate and the infinite beam are joined along the line $y = 0$, a force per unit length $f_1(x)$ acts between them as shown in Figure 37. It is assumed that the external point force is only acting on the beam located at $y = 0$ (beam 1). The force is defined by $\tilde{F}_0\delta(x-0)$. Now considering all forces related to the beam 1, the motion of this beam with damping becomes

$$\tilde{D}_{b1}\frac{\partial^4 \tilde{w}_{b1}(x)}{\partial x^4} - m'_{b1}\omega^2 \tilde{w}_{b1}(x) = \tilde{F}_0\delta(x-0) - \tilde{f}_1(x) \qquad (7.1)$$

where subscript $b1$ stands for the beam 1 and therefore, $\tilde{D}_{b1}$ is its bending stiffness and m'_{b1} is its mass per unit length. In the same manner, the equation of motion for the other beam (beam 2) is

$$\tilde{D}_{b2}\frac{\partial^4 \tilde{w}_{b2}(x)}{\partial x^4} - m'_{b2}\omega^2 \tilde{w}_{b2}(x) = \tilde{f}_2(x)\,. \tag{7.2}$$

Therefore, the spatial Fourier transform of equations (7.1) and (7.2) gives respectively

$$\tilde{D}_{b1}k_x^4 \tilde{W}_{b1}(k_x) - m'_{b1}\omega^2 \tilde{W}_{b1}(k_x) = \tilde{F}_0 - \tilde{F}_1(k_x)\,, \tag{7.3}$$

$$\tilde{D}_{b2}k_x^4 \tilde{W}_{b2}(k_x) - m'_{b2}\omega^2 \tilde{W}_{b2}(k_x) = \tilde{F}_2(k_x) \tag{7.4}$$

where $\tilde{F}_1(k_x)$ and $\tilde{F}_2(k_x)$ are the Fourier transforms of $\tilde{f}_1(x)$ and $\tilde{f}_2(x)$ respectively.

The equation of motion of the free plate with damping is the same as shown in the earlier section (equation (2.7)).

$$\tilde{D}_p\left(\frac{\partial^4 \tilde{w}_p(x,y)}{\partial x^4} + 2\frac{\partial^4 \tilde{w}_p(x,y)}{\partial x^2 \partial y^2} + \frac{\partial^4 \tilde{w}_p(x,y)}{\partial y^4}\right) - m''_p\omega^2 \tilde{w}_p(x,y) = 0\,, \tag{7.5}$$

and the corresponding Fourier transform of equation (7.5) is

$$\tilde{D}_p\left\{k_x^4 \tilde{W}_p(k_x,y) - 2k_x^2\frac{\partial^2 \tilde{W}_p(k_x,y)}{\partial y^2} + \frac{\partial^4 \tilde{W}_p(k_x,y)}{\partial y^4}\right\} - m'_p\omega^2 \tilde{W}_p(k_x,y) = 0\,. \tag{7.6}$$

Supposing the solution for the harmonic wave in the plate $w_p(y) = \tilde{B}e^{k_y y}$, the wavenumber relationship can be determined as before. Then, the waves in the plate propagating or decaying away from the junction of beam 1 and the plate are found to have the following wavenumbers.

$$k_y = -\sqrt{k_x^2 - \tilde{k}_p^2} = \tilde{k}_{y1}\,, \tag{7.7a}$$

$$k_y = -\sqrt{k_x^2 + \tilde{k}_p^2} = \tilde{k}_{y2}\,. \tag{7.7b}$$

Meanwhile, the positive square roots are assumed for waves travelling towards the junction of beam 1 and the plate and are found to be

$$k_y = \sqrt{k_x^2 - \tilde{k}_p^2} = \tilde{k}_{y3}, \tag{7.7c}$$

$$k_y = \sqrt{k_x^2 + \tilde{k}_p^2} = \tilde{k}_{y4}. \tag{7.7d}$$

If $|k_x| < |\tilde{k}_p|$, then wavenumbers $\tilde{k}_{y1}$ and $\tilde{k}_{y3}$ are considered as travelling waves, and $\tilde{k}_{y2}$ and $\tilde{k}_{y4}$ are considered as nearfield waves. Conversely, if $|k_x| > |\tilde{k}_p|$, then all of them behave as nearfield waves.

Consequently the motion of the plate can be written as

$$\tilde{W}_p(k_x, y) = \tilde{B}_1 e^{\tilde{k}_{y1} y} + \tilde{B}_2 e^{\tilde{k}_{y2} y} + \tilde{B}_3 e^{\tilde{k}_{y3} y} + \tilde{B}_4 e^{\tilde{k}_{y4} y} \tag{7.8}$$

where each wavenumber is calculated in equation (7.7).

Based on the wavenumbers obtained, the response of the beams and the plate can be identified. This procedure starts initially from the boundary conditions. All boundary conditions related to the beams and plate are as follows.

(i) Continuity equation for beam 1 and beam 2; equal displacement to the plate at junctions $y = 0$ and $y = L_y$ respectively

$$\tilde{W}_{b1}(k_x) = \tilde{W}_p(k_x, y)\Big|_{y=0} \tag{7.9}$$

$$\tilde{W}_{b2}(k_x) = \tilde{W}_p(k_x, y)\Big|_{y=L_y} \tag{7.10}$$

Thus,

$$\tilde{W}_{b1}(k_x) = \tilde{B}_1 + \tilde{B}_2 + \tilde{B}_3 + \tilde{B}_4. \tag{7.11}$$

$$\tilde{W}_{b2}(k_x) = \tilde{B}_1 e^{\tilde{k}_{y1} L_y} + \tilde{B}_2 e^{\tilde{k}_{y2} L_y} + \tilde{B}_3 e^{\tilde{k}_{y3} L_y} + \tilde{B}_4 e^{\tilde{k}_{y4} L_y}. \tag{7.12}$$

(ii) Sliding condition; the beams are assumed infinitely stiff to torsion along $y=0$ and $y=L_y$

$$\left.\frac{\partial \tilde{W}_p(k_x,y)}{\partial y}\right|_{y=0}=0 \tag{7.13}$$

$$\left.\frac{\partial \tilde{W}_p(k_x,y)}{\partial y}\right|_{y=L_y}=0 \tag{7.14}$$

Therefore,

$$\left.\frac{\partial \tilde{W}_p(k_x,y)}{\partial y}\right|_{y=0}=\tilde{B}_1\tilde{k}_{y1}+\tilde{B}_2\tilde{k}_{y2}+\tilde{B}_3\tilde{k}_{y3}+\tilde{B}_4\tilde{k}_{y4}=0. \tag{7.15}$$

$$\left.\frac{\partial \tilde{W}_p(k_x,y)}{\partial y}\right|_{y=L_y}=\tilde{B}_1\tilde{k}_{y1}e^{\tilde{k}_{y1}L_y}+\tilde{B}_2\tilde{k}_{y2}e^{\tilde{k}_{y2}L_y}+\tilde{B}_3\tilde{k}_{y3}e^{\tilde{k}_{y3}L_y}+\tilde{B}_4\tilde{k}_{y4}e^{\tilde{k}_{y4}L_y}=0. \tag{7.16}$$

(iii) Force equilibrium condition; the forces on the plate are equal and opposite to the respective forces on the beams

$$\tilde{D}_p\left[\frac{\partial^3 \tilde{W}_p(k_x,y)}{\partial y^3}-k_x^2(2-\nu)\frac{\partial \tilde{W}_p(k_x,y)}{\partial y}\right]_{y=0}=\tilde{F}_1(k_x) \tag{7.17}$$

$$-\tilde{D}_p\left[\frac{\partial^3 \tilde{W}_p(k_x,y)}{\partial y^3}-k_x^2(2-\nu)\frac{\partial \tilde{W}_p(k_x,y)}{\partial y}\right]_{y=L_y}=-\tilde{F}_2(k_x) \tag{7.18}$$

Note that here, the negative sign of $\tilde{F}_2(k_x)$ is used to show the force relationship according to equation (7.4). As $\partial \tilde{W}_p(k_x,y)/\partial y=0$ from equations (7.13) and (7.14), equations (7.17) and (7.18) become respectively

$$\tilde{D}_p\left[\frac{\partial^3 \tilde{W}_p(k_x,y)}{\partial y^3}\right]_{y=0}=\tilde{D}_p\left[\tilde{B}_1\tilde{k}_{y1}^3+\tilde{B}_2\tilde{k}_{y2}^3+\tilde{B}_3\tilde{k}_{y3}^3+\tilde{B}_4\tilde{k}_{y4}^3\right]=\tilde{F}_1(k_x), \tag{7.19}$$

$$\tilde{D}_p\left[\frac{\partial^3 \tilde{W}_p(k_x,y)}{\partial y^3}\right]_{y=L_y}=\tilde{D}_p\left[\tilde{B}_1\tilde{k}_{y1}^3e^{\tilde{k}_{y1}L_y}+\tilde{B}_2\tilde{k}_{y2}^3e^{\tilde{k}_{y2}L_y}+\tilde{B}_3\tilde{k}_{y3}^3e^{\tilde{k}_{y3}L_y}+\tilde{B}_4\tilde{k}_{y4}^3e^{\tilde{k}_{y4}L_y}\right]=\tilde{F}_2(k_x). \tag{7.20}$$

By introducing a matrix form, the above equations can be written simply as

$$\begin{Bmatrix} \tilde{W}_{b1}(k_x) \\ \tilde{W}_{b2}(k_x) \\ 0 \\ 0 \end{Bmatrix} = \begin{bmatrix} 1 & 1 & 1 & 1 \\ e^{\tilde{k}_{y1}L_y} & e^{\tilde{k}_{y2}L_y} & e^{\tilde{k}_{y3}L_y} & e^{\tilde{k}_{y4}L_y} \\ \tilde{k}_{y1} & \tilde{k}_{y2} & \tilde{k}_{y3} & \tilde{k}_{y4} \\ \tilde{k}_{y1}e^{\tilde{k}_{y1}L_y} & \tilde{k}_{y2}e^{\tilde{k}_{y2}L_y} & \tilde{k}_{y3}e^{\tilde{k}_{y3}L_y} & \tilde{k}_{y4}e^{\tilde{k}_{y4}L_y} \end{bmatrix} \begin{Bmatrix} \tilde{B}_1 \\ \tilde{B}_2 \\ \tilde{B}_3 \\ \tilde{B}_4 \end{Bmatrix}, \tag{7.21}$$

and

$$\begin{Bmatrix} \tilde{F}_1(k_x) \\ \tilde{F}_2(k_x) \end{Bmatrix} = \begin{bmatrix} \tilde{D}_p\tilde{k}_{y1}^3 & \tilde{D}_p\tilde{k}_{y2}^3 & \tilde{D}_p\tilde{k}_{y3}^3 & \tilde{D}_p\tilde{k}_{y4}^3 \\ \tilde{D}_p\tilde{k}_{y1}^3 e^{\tilde{k}_{y1}L_y} & \tilde{D}_p\tilde{k}_{y2}^3 e^{\tilde{k}_{y2}L_y} & \tilde{D}_p\tilde{k}_{y3}^3 e^{\tilde{k}_{y3}L_y} & \tilde{D}_p\tilde{k}_{y4}^3 e^{\tilde{k}_{y4}L_y} \end{bmatrix} \begin{Bmatrix} \tilde{B}_1 \\ \tilde{B}_2 \\ \tilde{B}_3 \\ \tilde{B}_4 \end{Bmatrix}. \tag{7.22}$$

Equation (7.21) can be transformed, using inverse notation, into

$$\begin{Bmatrix} \tilde{B}_1 \\ \tilde{B}_2 \\ \tilde{B}_3 \\ \tilde{B}_4 \end{Bmatrix} = \begin{bmatrix} 1 & 1 & 1 & 1 \\ e^{\tilde{k}_{y1}L_y} & e^{\tilde{k}_{y2}L_y} & e^{\tilde{k}_{y3}L_y} & e^{\tilde{k}_{y4}L_y} \\ \tilde{k}_{y1} & \tilde{k}_{y2} & \tilde{k}_{y3} & \tilde{k}_{y4} \\ \tilde{k}_{y1}e^{\tilde{k}_{y1}L_y} & \tilde{k}_{y2}e^{\tilde{k}_{y2}L_y} & \tilde{k}_{y3}e^{\tilde{k}_{y3}L_y} & \tilde{k}_{y4}e^{\tilde{k}_{y4}L_y} \end{bmatrix}^{-1} \begin{Bmatrix} \tilde{W}_{b1}(k_x) \\ \tilde{W}_{b2}(k_x) \\ 0 \\ 0 \end{Bmatrix}. \tag{7.23}$$

Substituting equation (7.23) into equation (7.22) gives

$$\begin{aligned} &\begin{Bmatrix} \tilde{F}_1(k_x) \\ \tilde{F}_2(k_x) \end{Bmatrix} \\ &= \begin{bmatrix} \tilde{D}_p\tilde{k}_{y1}^3 & \tilde{D}_p\tilde{k}_{y2}^3 & \tilde{D}_p\tilde{k}_{y3}^3 & \tilde{D}_p\tilde{k}_{y4}^3 \\ \tilde{D}_p\tilde{k}_{y1}^3 e^{\tilde{k}_{y1}L_y} & \tilde{D}_p\tilde{k}_{y2}^3 e^{\tilde{k}_{y2}L_y} & \tilde{D}_p\tilde{k}_{y3}^3 e^{\tilde{k}_{y3}L_y} & \tilde{D}_p\tilde{k}_{y4}^3 e^{\tilde{k}_{y4}L_y} \end{bmatrix} \\ &\times \begin{bmatrix} 1 & 1 & 1 & 1 \\ e^{\tilde{k}_{y1}L_y} & e^{\tilde{k}_{y2}L_y} & e^{\tilde{k}_{y3}L_y} & e^{\tilde{k}_{y4}L_y} \\ \tilde{k}_{y1} & \tilde{k}_{y2} & \tilde{k}_{y3} & \tilde{k}_{y4} \\ \tilde{k}_{y1}e^{\tilde{k}_{y1}L_y} & \tilde{k}_{y2}e^{\tilde{k}_{y2}L_y} & \tilde{k}_{y3}e^{\tilde{k}_{y3}L_y} & \tilde{k}_{y4}e^{\tilde{k}_{y4}L_y} \end{bmatrix}^{-1} \begin{Bmatrix} \tilde{W}_{b1}(k_x) \\ \tilde{W}_{b2}(k_x) \\ 0 \\ 0 \end{Bmatrix}. \end{aligned} \tag{7.24}$$

To simplify this equation, new variables σ and τ are introduced so that equation (7.24) becomes

$$\begin{Bmatrix} \tilde{F}_1(k_x) \\ \tilde{F}_2(k_x) \end{Bmatrix} = \begin{bmatrix} \sigma_1 & \sigma_2 & \sigma_3 & \sigma_4 \\ \tau_1 & \tau_2 & \tau_3 & \tau_4 \end{bmatrix} \begin{Bmatrix} \tilde{W}_{b1}(k_x) \\ \tilde{W}_{b2}(k_x) \\ 0 \\ 0 \end{Bmatrix} \tag{7.25}$$

where

$$\begin{bmatrix} \sigma_1 & \sigma_2 & \sigma_3 & \sigma_4 \\ \tau_1 & \tau_2 & \tau_3 & \tau_4 \end{bmatrix}$$

$$= \tilde{D}_p \begin{bmatrix} \tilde{k}_{y1}^3 & \tilde{k}_{y2}^3 & \tilde{k}_{y3}^3 & \tilde{k}_{y4}^3 \\ \tilde{k}_{y1}^3 e^{\tilde{k}_{y1}L_y} & \tilde{k}_{y2}^3 e^{\tilde{k}_{y2}L_y} & \tilde{k}_{y3}^3 e^{\tilde{k}_{y3}L_y} & \tilde{k}_{y4}^3 e^{\tilde{k}_{y4}L_y} \end{bmatrix} \begin{bmatrix} 1 & 1 & 1 & 1 \\ e^{\tilde{k}_{y1}L_y} & e^{\tilde{k}_{y2}L_y} & e^{\tilde{k}_{y3}L_y} & e^{\tilde{k}_{y4}L_y} \\ \tilde{k}_{y1} & \tilde{k}_{y2} & \tilde{k}_{y3} & \tilde{k}_{y4} \\ \tilde{k}_{y1} e^{\tilde{k}_{y1}L_y} & \tilde{k}_{y2} e^{\tilde{k}_{y2}L_y} & \tilde{k}_{y3} e^{\tilde{k}_{y3}L_y} & \tilde{k}_{y4} e^{\tilde{k}_{y4}L_y} \end{bmatrix}^{-1}.$$

Note that σ and τ are related only to the plate properties. Equation (7.25), describing the relationship between the forces $\tilde{F}(k_x)$ and the displacements $\tilde{W}_b(k_x)$, can be written simply as

$$\begin{Bmatrix} \tilde{F}_1(k_x) \\ \tilde{F}_2(k_x) \end{Bmatrix} = \begin{bmatrix} \sigma_1 & \sigma_2 \\ \tau_1 & \tau_2 \end{bmatrix} \begin{Bmatrix} \tilde{W}_{b1}(k_x) \\ \tilde{W}_{b2}(k_x) \end{Bmatrix}. \tag{7.26}$$

Substituting equation (7.26) into equations (7.3) and (7.4), gives

$$\tilde{D}_{b1} k_x^4 \tilde{W}_{b1}(k_x) - m'_{b1}\omega^2 \tilde{W}_{b1}(k_x) = \tilde{F}_0 - \left[\sigma_1 \tilde{W}_{b1}(k_x) + \sigma_2 \tilde{W}_{b2}(k_x)\right], \tag{7.27}$$

and

$$\tilde{D}_{b2} k_x^4 \tilde{W}_{b2}(k_x) - m'_{b2}\omega^2 \tilde{W}_{b2}(k_x) = \left[\tau_1 \tilde{W}_{b1}(k_x) + \tau_2 \tilde{W}_{b2}(k_x)\right]. \tag{7.28}$$

Again, equations (7.27) and (7.28) can be written in matrix form as

$$\begin{bmatrix} \tilde{D}_{b1} k_x^4 - m'_{b1}\omega^2 + \sigma_1 & \sigma_2 \\ -\tau_1 & \tilde{D}_{b2} k_x^4 - m'_{b2}\omega^2 - \tau_2 \end{bmatrix} \begin{Bmatrix} \tilde{W}_{b1}(k_x) \\ \tilde{W}_{b2}(k_x) \end{Bmatrix} = \begin{Bmatrix} \tilde{F}_0 \\ 0 \end{Bmatrix}. \tag{7.29}$$

As $m'_{b1}\omega^2 / \tilde{D}_{b1} = \tilde{k}_{b1}^4$ and $m'_{b2}\omega^2 / \tilde{D}_{b2} = \tilde{k}_{b2}^4$, equation (7.29) is

$$\begin{bmatrix} k_x^4 - \tilde{k}_{b1}^4 + \sigma_1 / \tilde{D}_{b1} & \sigma_2 / \tilde{D}_{b1} \\ -\tau_1 / \tilde{D}_{b2} & k_x^4 - \tilde{k}_{b2}^4 - \tau_2 / \tilde{D}_{b2} \end{bmatrix} \begin{Bmatrix} \tilde{W}_{b1}(k_x) \\ \tilde{W}_{b2}(k_x) \end{Bmatrix} = \begin{Bmatrix} \tilde{F}_0 / \tilde{D}_{b1} \\ 0 \end{Bmatrix}. \tag{7.30}$$

Finally, by inverting this equation the response of beam 1 can be expressed as

$$\tilde{W}_{b1}(k_x) = \frac{\tilde{F}_0}{\tilde{D}_{b1}} \frac{k_x^4 - \tilde{k}_{b2}^4 - \tau_2 / \tilde{D}_{b2}}{\left(k_x^4 - \tilde{k}_{b1}^4 + \sigma_1 / \tilde{D}_{b1}\right)\left(k_x^4 - \tilde{k}_{b2}^4 - \tau_2 / \tilde{D}_{b2}\right) + \sigma_2 \tau_1 / \left(\tilde{D}_{b1} \tilde{D}_{b2}\right)}. \tag{7.31}$$

Accordingly, the response of beam 2 becomes

$$\tilde{W}_{b2}(k_x) = \frac{\tau_1 / \tilde{D}_{b2}}{k_x^4 - \tilde{k}_{b2}^4 - \tau_2 / \tilde{D}_{b2}} \tilde{W}_{b1}(k_x). \tag{7.32}$$

The responses $w_{b1}(x)$ and $w_{b2}(x)$ can be obtained from the inverse Fourier transform of these equations according to equation (2.4). More over from $\tilde{W}_{b1}(k_x)$ and $\tilde{W}_{b2}(k_x)$, equation (7.23) can be used to find $\tilde{B}_1$, $\tilde{B}_2$, $\tilde{B}_3$ and $\tilde{B}_4$. These can then be substituted into equation (7.8) to give $\tilde{W}_p(k_x, y)$ which can be inverse Fourier transformed to give $\tilde{w}_p(x, y)$.

7.2 Response of two-beam structure consisting of finite beams

Consider the coupled structure shown in Figure 38 where the ends of both finite beams are considered to be sliding. Accordingly, the two corresponding edges of the plate are also assumed to be sliding. As before, the beams are assumed to have infinite torsional stiffness and it is arranged that the neutral axis lies in the centre of the beams.

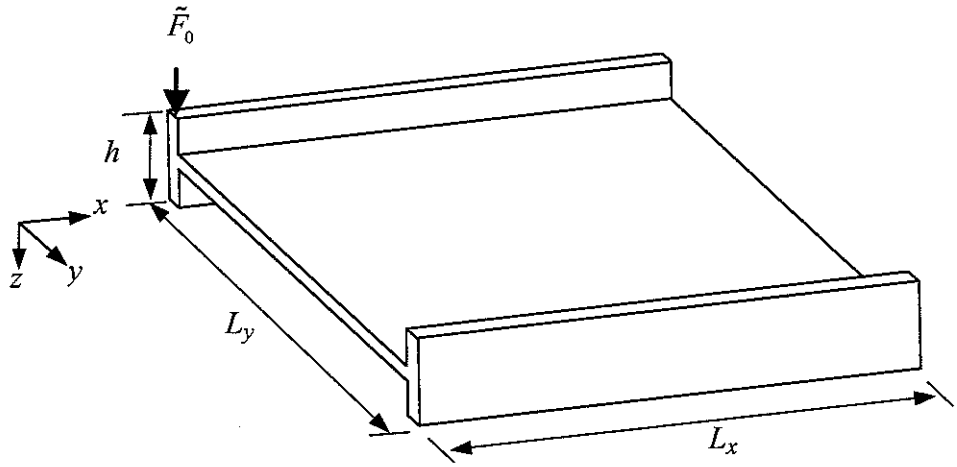

Figure 38. A built-up structure consisting of two finite beams attached to a rectangular plate.

As explained in section 4.1, the behaviour of the coupled beams with sliding conditions can be described in terms of cosine orders. Therefore, the motion of the coupled beam 1 is written as

$$\tilde{w}_{b1}(x) = \frac{\tilde{W}_{b1,0}}{2} + \sum_{n=1}^{\infty} \tilde{W}_{b1,n} \cos(k_{x,n} x) \tag{7.33}$$

where $k_{x,n} = n\pi / L_x$ and $\tilde{W}_{b1,n} = \tilde{W}_{b1}(k_{x,n})$ is the n^{th} component of the motion of the coupled beam 1, which is defined in equation (7.31). Also the response of the coupled beam 2 is

$$\tilde{w}_{b2}(x) = \frac{\tilde{W}_{b2,0}}{2} + \sum_{n=1}^{\infty} \tilde{W}_{b2,n} \cos(k_{x,n} x). \tag{7.34}$$

The motion of the plate can also be written in terms of the Fourier series as

$$\tilde{w}_p(x,y) = \frac{\tilde{W}_{p,0}(y)}{2} + \sum_{n=1}^{\infty} \tilde{W}_{p,n}(y)\cos(k_{x,n}x) \qquad (7.35)$$

where $\tilde{W}_{p,n}(y) = \tilde{W}_p(k_{x,n}, y)$ is the n^{th} component of the motion of the plate, presented in equation (7.8).

7.3 Power balance of the subsystems

The power balance explained in section 4.2 can be applied to the coupled structure consisting of two beams and a plate shown in Figure 38. The power relationship can be represented using the power flow between subsystems as shown in Figure 39, where, for example $P_{b1\to p}$ means the power transferred from beam 1 to the plate and $P_{b1,dis}$ is the power dissipated in beam 1.

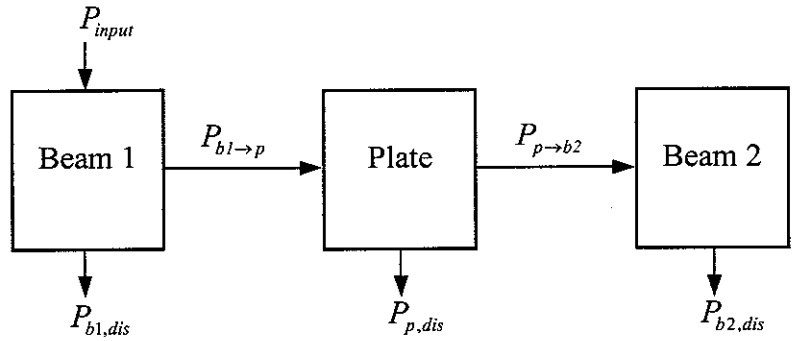

Figure 39. Power balance between subsystems of the coupled structure as in Figure 38.

The power flows such as $P_{b1\to p}$ represent the net power transferred between the subsystems. The power balance between the input and output power with respect to any subsystem should hold; this will be verified in a numerical example later. Most of the equations used for obtaining the transferred power and the dissipated power for a subsystem are the same as presented in section 4.2, except for the response of the plate. The difference for the plate response is due to the different notation in equations (3.1) and (7.8).

7.4 Numerical analysis

Using the Fourier series, the response of the beam-plate-beam structure shown in Figure 38 is calculated. The width of the plate L_y is 1.5 m and all other material properties and dimensions are the same as given in Table 2. The plate is connected to the centre of the beams. Although the mathematical development allows the two beams to have different

properties, for the purpose of validation the two beams are here taken to be identical. In the Fourier series 400 components ($n = 400$) are considered which approximately corresponds to the non-dimensional wavenumber $\gamma = 50$ at 1 kHz.

Firstly, the point mobility at one end of the beam is presented in Figure 40. The result shows excellent agreement with that of FEM. Also, as shown in Figure 41, the transfer mobility to a point $x = 1.51$ m and $y = 0.99$ m on the plate agrees well with that obtained using FEM.

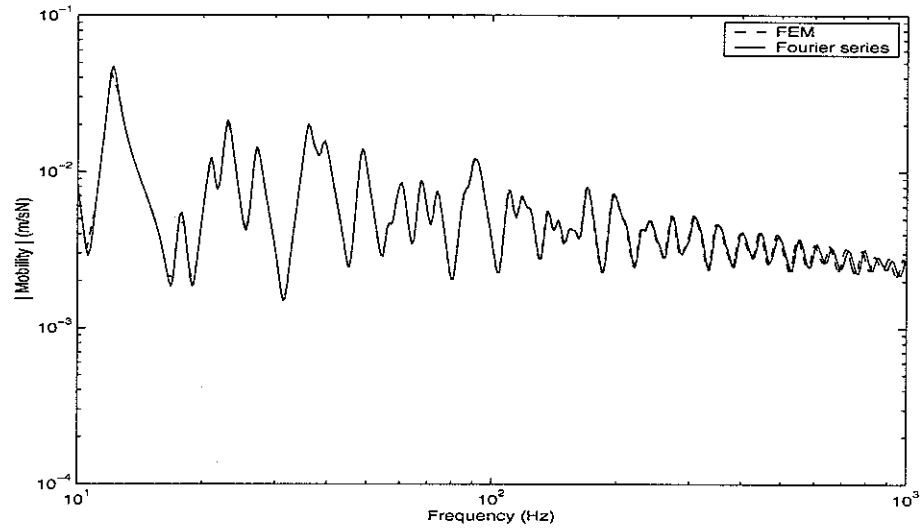

Figure 40. Point mobility of the built-up structure as in Figure 38 ($\eta_p = 0.05$ in the plate, $\eta_b = 0.05$ in the beam, point force applied at $x = 0$ of beam 1).

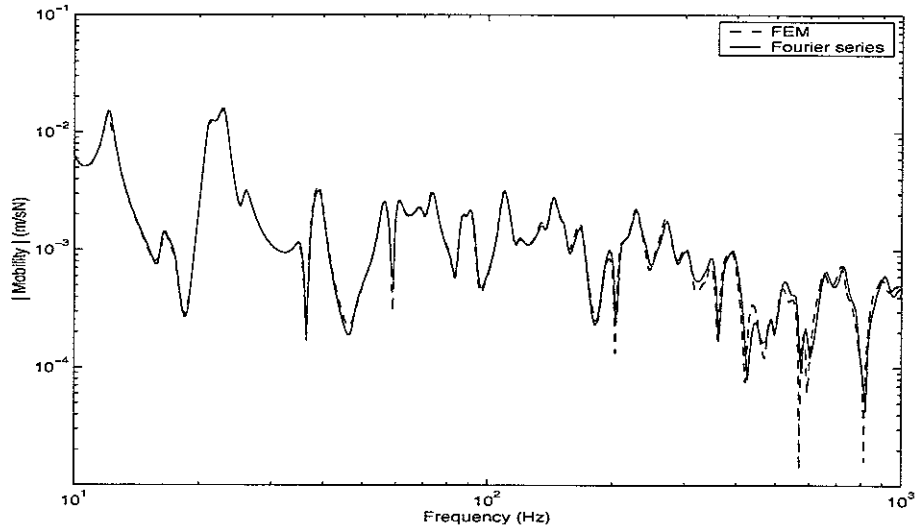

Figure 41. Transfer mobility for the built-up structure (Figure 38) to a point at the plate (at $x = 1.51$ m and $y = 0.99$ m, $\eta_p = 0.05$ in the plate, $\eta_b = 0.05$ in the beam, point force applied at $x = 0$ of beam 1).

The powers related to the subsystems are compared from the point of view of the power balance shown in Figure 39. Figure 42 shows the total power and the net power transferred between subsystems. From the two transferred powers, it can be inferred that the difference between them is the dissipated power in the plate.

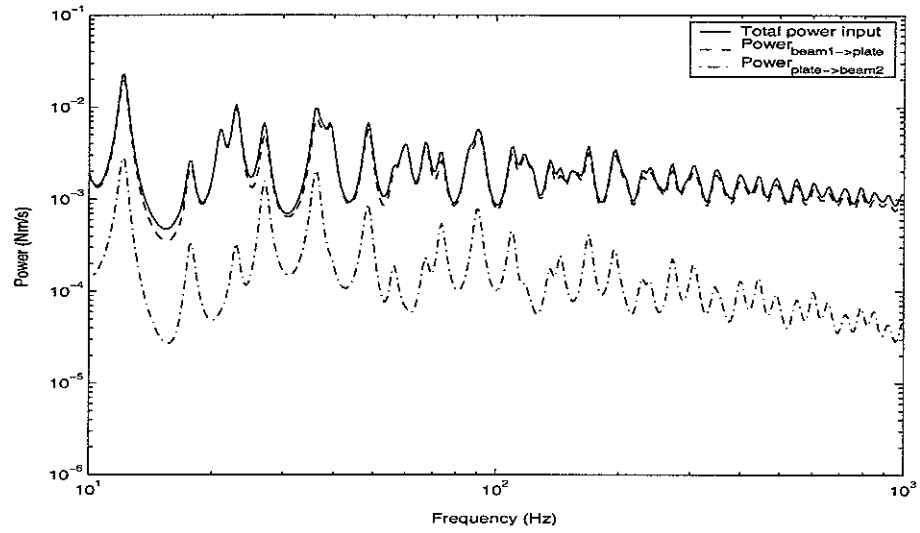

Figure 42. Comparison of total input power to the built-up structure as in Figure 38, the net power transferred to the plate and the net power from the plate to the second beam ($\eta_p = 0.05$ in the plate, $\eta_b = 0.05$ in the beam, point force applied at $x = 0$ of beam 1).

The power input and output (dissipated plus transferred) for beam 1 are shown in Figure 43, which indicate that the power balance is maintained (maximum error of 0.1 %).

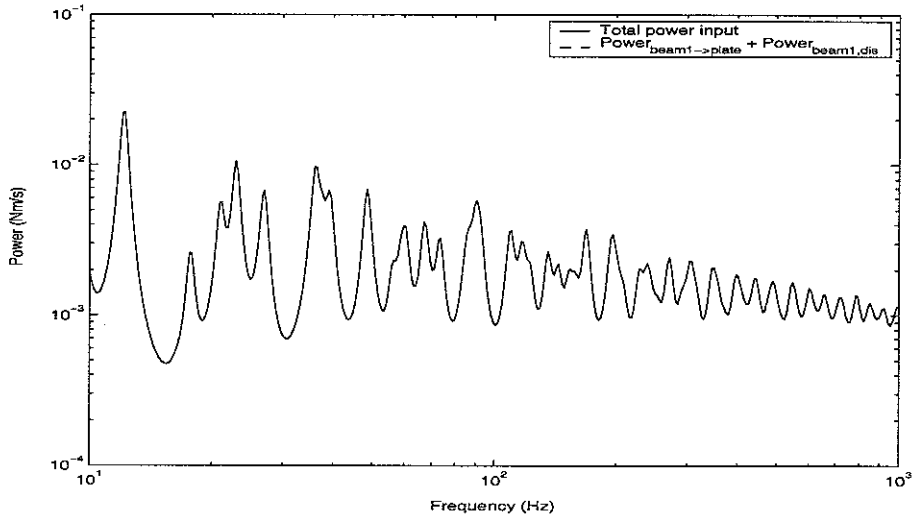

Figure 43. Comparison of power balance for beam 1 ($\eta_p = 0.05$ in the plate, $\eta_b = 0.05$ in the beam, point force applied at $x = 0$ of beam 1).

In the same way, the powers related to the plate and beam 2 are shown in Figure 44 and Figure 45 respectively. Good agreement can be seen between the input and output power in each case (maximum error of 0.6 % and 0.0 % respectively). Note in the previous wave analysis [1], the power quantities related to beam 2 showed small differences at some frequencies, as the power calculation was based on a synthesis of the anti-symmetric and the symmetric response using the wave method for the plate the power balance was found to be violated. Considering the good agreement of the power balance for all subsystems, here the Fourier series method seems to be appropriate for obtaining the correct response of the coupled structure such as the beam-plate-beam structure.

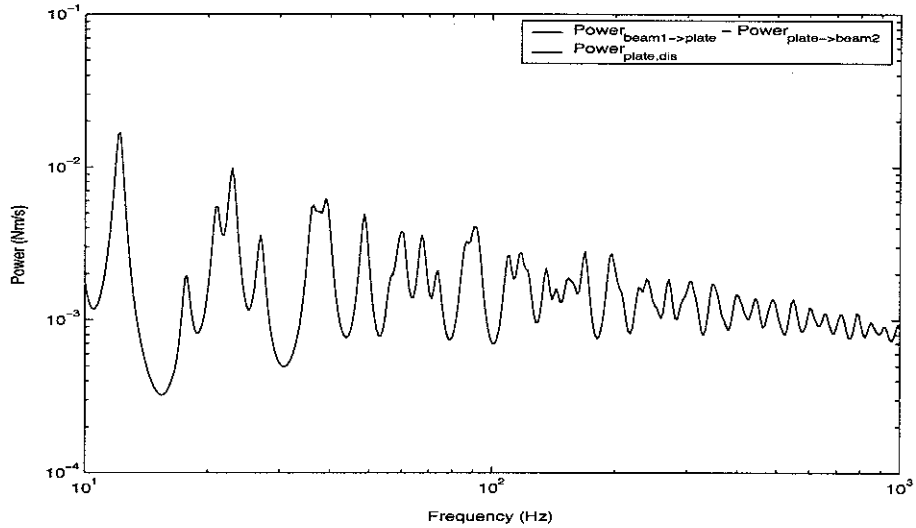

Figure 44. Comparison of power balance for the plate ($\eta_p = 0.05$ in the plate, $\eta_b = 0.05$ in the beam, point force applied at $x = 0$ of beam 1).

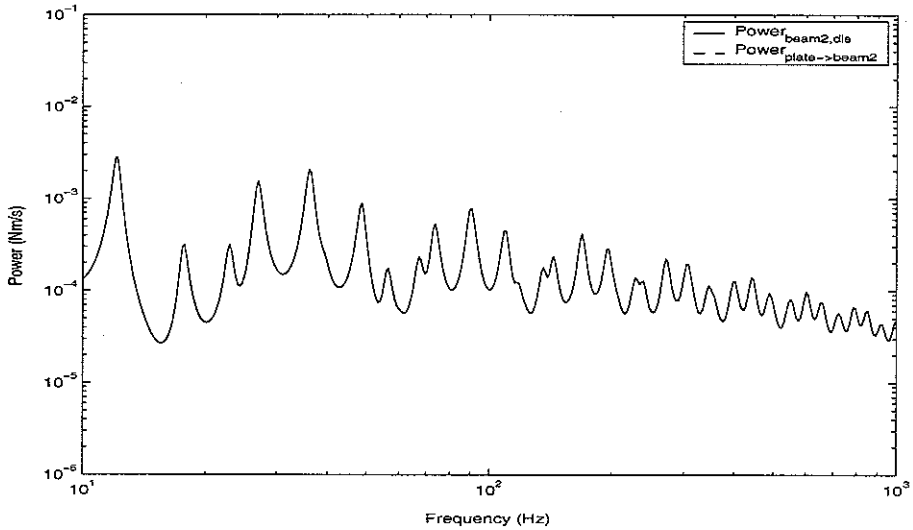

Figure 45. Comparison of power balance for beam 2 ($\eta_p = 0.05$ in the plate, $\eta_b = 0.05$ in the beam, point force applied at $x = 0$ of beam 1).

8. CONCLUSIONS

In the present report, the Fourier transform and Fourier series methods are used to analyse the structural behaviour of a coupled beam-plate structure and a beam-plate-beam structure and numerical results are compared with FE analysis.

Firstly, for the case where a beam is excited by an external force, the Fourier transformed motion of the infinite coupled beam is developed when an infinite plate is attached to the beam. From the coupled equations of the motion, the influence of the plate on the beam is identified in the wavenumber domain. The damping effect as well as the mass effect of the plate is identified and explained. It has been shown that the mass effect becomes smaller as frequency increases due to a term $1/k_p$. Also, comparing the response of the coupled beam obtained using the FFT, it has been highlighted that the effective damping due to the plate decreases as frequency increases. These structural influences of the plate on the beam agree with those explained and described previously [1, 3].

Although the Fourier transform method should consider all possible wavenumbers k_x, this is not realistic or possible. Therefore, a consistent rule for truncating the sufficiently low level response with respect to the maximum response (60 dB) is used. The numerical analysis based on this rule for the coupled structure produces accurate numerical results.

To obtain the response of a coupled structure consisting of a finite beam and a finite width plate a Fourier series method has been developed and implemented. Accordingly, equations for power identification of the coupled structure are presented based on the Fourier series. Comparing the numerical results with those of FEM, very good agreement is found. Also, investigation of the power balance showed that the violation of the energy conservation for the finite plate found previously using the wave method [3] was overcome. The Fourier approach could therefore be a good method to analyse the behaviour of such a finite coupled structure.

The coupled structure consisting of a beam and a plate is also investigated in terms of the Fourier technique where the plate is excited. The numerical results show good agreement with those of FEM. It is also shown that the principle of reciprocity holds by comparing the transfer mobilities where the external point force is applied on the beam or on the plate. The power balance is also in good agreement for this case.

Previously [3], a more complicated structure such as a beam-plate-beam structure was studied using the wave method, from which it was shown that the wave method had some

limitations because the response is obtained based on an anti-symmetric and a symmetric response of a beam-plate structure. However, the developments in the present report show that the Fourier approach is applicable for the analysis of the beam-plate-beam structure. This is confirmed by applying the technique to the same symmetric structure presented previously [3]. The transfer mobility as well as the point mobility show very good agreement with those of FEM. Also the power balance is maintained between the substructures. The formulation developed can also be applied to non-symmetric beam-plate-beam system and this will be examined further in future study.

The method developed in this report can be used to study the coupling between a bema and a plate in terms of Statistical Energy Analysis (SEA). This wll form the subject of a subsequent report.

References

1. J. W. Yoo, D. J. Thompson and N. S. Ferguson 2003 *ISVR Memorandom No*: **905**. Structural analysis of a symmetric structure consisting of two beams and a plate based on a wave approach.

2. L. Ji, B. R. Mace and R. J. Pinnington 2002 *ISVR Memorandom No*: **876**. Power transmission to flexible receivers by force sources.

3. J. W. Yoo, N. S. Ferguson and D. J. Thompson 2002 *ISVR Memorandom No*: **888**. Structural analysis of a combined beam and plate structure using a wave approach.

4. E. Kreyszig 1983 *Advanced engineering mathematics*. New York: John Wiley & Sons; fifth edition.

5. L. Cremer, M. Heckl and E. E. Ungar 1988 *Structure-borne Sound*. Berlin: Springer Verlag; 2nd edition.

6. R. M. Grice and R. J. Pinnington 1999 *Journal of Sound and Vibration* **230**, 825-849. A method for the vibrational analysis of built-up structures, part 1: Introduction and analytical analysis of the plate-stiffened beam.

7. The Math Works, Inc. 2001, *MATLAB Function Reference Volume 3: P – Z (on line version)*.

8. R. W. Ramirez 1985 *The FFT Fundamentals and Concepts*. N. J.: Prentice-Hall.

9. M. Petyt 1990 *Introduction to finite element vibration analysis*. Cambridge: Cambridge University Press.

10. R. H. Lyon and R. G. Dejong 1995 *Theory and Application of Statistical Energy Analysis*. Boston: Butterworth-Heinemann.

11. G. B. Warburton 1976 *The Dynamical Behaviour of Structures*. Oxford: Pergamon Press; second edition.

12 W. S. Park 2002 *PhD Thesis, University of Southampton*. The sources of variability in statistical energy analysis coupling of two rectangular plates.

13. F. Fahy and J. Walker 1998 *Fundamentals of noise and vibration*, London: E & FN Spon.

14. S. P. Timoshenko and S. Woinowsky-Krieger 1959 *Theory of plates and shells*, New York: McGraw-Hill; second edition.

Appendix. Nomenclature

B	wave amplitude in a plate (m)
C	wave amplitude in a plate (m)
D	beam bending stiffness (Nm^2); plate bending stiffness (Nm)
E	Young's modulus of elasticity (N/m^2); energy (J)
F	force per unit length (N/m)
L_x	length of a beam (m)
L_y	width of a plate (m)
P	power (Watt)
Z'	structural impedance per unit length (Ns/m^2)
f	frequency (Hz); force (N)
h	height of a beam (m)
i	$\sqrt{-1}$
k_b	uncoupled beam wavenumber (rad/m)
$k_{x,n}$	$n\pi/L_x$
k_p	uncoupled free wavenumber in a plate
k_x	coupled travelling trace wavenumber of a beam
k_y	trace wavenumber in a plate
m_b'	mass per unit length of a beam (kg/m)
m_p''	mass per unit area of a plate (kg/m^2)
$\tilde{r}$	reflection coefficient (-)
t	thickness (m); time (s)
w	displacement (m)
x, y, z	co-ordinates (m)
α	constant
β	constant
$\tilde{\beta}$	travelling wave attenuation coefficient (-)

γ	non-dimensional wavenumber ($= k_x / k_b$)
δ	Dirac delta function
η	structural loss factor (-)
ν	Poisson's ratio
ξ	non-dimensional wavenumber ($= k_b / \tilde{k}_p$)
ρ	density (kg/m^3)
σ	constant
τ	constant
ω	radian frequency (rad/s)
ϕ	$\sqrt{(\gamma\xi)^2 + 1}$
ψ	$\sqrt{(\gamma\xi)^2 - 1}$
μ	$m_p'' / (m_b' k_p)$